AFML-TR-65-2
PART I, VOLUME XIII

TERNARY PHASE EQUILIBRIA IN TRANSITION METAL-BORON-CARBON-SILICON SYSTEMS

PART I. BINARY SYSTEMS
Volume XIII. The Zirconium-Silicon and Hafnium-Silicon Systems

C. E. BRUKL

AEROJET-GENERAL CORPORATION

TECHNICAL REPORT AFML-TR-65-2, PART I, VOLUME XIII

MAY 1968

AIR FORCE MATERIALS LABORATORY
AIR FORCE SYSTEMS COMMAND
WRIGHT-PATTERSON AIR FORCE BASE, OHIO

NOTICES

When Government drawings, specifications, or other data are used for any purpose other than in connection with a definitely related Government procurement operation, the United States Government thereby incurs no responsibility nor any obligation whatsoever; and the fact that the Government may have formulated, furnished, or in any way supplied the said drawings, specifications, or other data, is not to be regarded by implication or otherwise as in any manner licensing the holder or any other person or corporation, or conveying any rights or permission to manufacture, use, or sell any patented invention that may in any way be related thereto.

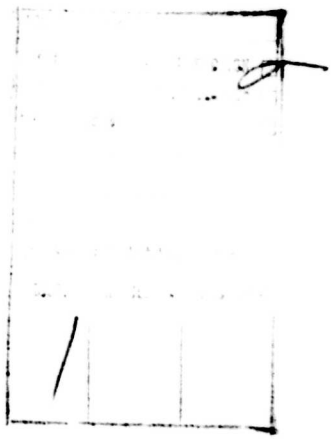

Copies of this report should not be returned unless return is required by security considerations, contractual obligations, or notice on a specific document.

400 - June 1968 - CO455 - 40-849

TERNARY PHASE EQUILIBRIA IN TRANSITION METAL-BORON-CARBON-SILICON SYSTEMS

PART I. BINARY SYSTEMS
Volume XIII. The Zirconium-Silicon and Hafnium-Silicon Systems

C. E. BRUKL

FOREWORD

The research described in this report was carried out at the Materials Research Laboratory, Aerojet-General Corporation, Sacramento, California, under USAF Contract No. AF 33(615)-1249. The contract was initiated under Project No. 7350, Task No. 735001, and was administered under the direction of the Air Force Materials Laboratory, with Lt. P.J. Marchiando acting as Project Engineer, and Dr. E. Rudy, Aerojet-General Corporation, as Principal Investigator. Professor Dr. Hans Nowotny, University of Vienna, served as consultant to the project.

The project, which includes the experimental and theoretical investigations of ternary and related binary systems in the system classes Me_1-Me_2-C, Me-B-C, Me_1-Me_2-B, Me-Si-B and Me-Si-C, was initiated on 1 January 1964. An extension effort to this contract commenced in January 1966.

The phase diagram work on the binary systems described in this report were carried out by C.E. Brukl. Assisting in the investigations were: J. Hoffman (metallographic preparations), J. Pomodoro (sample preparation), and R. Cobb (X-ray exposures and photographic work). The author wishes to thank Dr. E. Rudy for his assistance in interpretation of some of the metallographic specimens.

Chemical analysis of the alloys was performed under the supervision of Mr. W.E. Trahan, Quality Control Division of Aerojet-General Corporation. The author wishes to thank Mr. R. Cristoni for the preparation of the illustrations, and Mrs. J. Weidner, who typed the report.

The manuscript of this report was released by the author November 1967 for publication.

Other reports issued under USAF Contract AF 33(615)-1249 have included:

Part I. Related Binaries

Volume I.	Mo-C System
Volume II.	Ti-C and Zr-C Systems
Volume III.	Systems Mo-B and W-B
Volume IV.	Hf-C System
Volume V.	Ta-C System. Partial Investigations in the Systems V-C and Nb-C
Volume VI.	W-C System. Supplemental Information on the Mo-C System
Volume VII.	Ti-B System
Volume VIII.	Zr-B System
Volume IX.	Hf-B System
Volume X.	V-B, Nb-B, and Ta-B Systems
Volume XI.	Final Report on the Mo-C System
Volume XII.	Revision of the Vanadium-Carbon and Niobium-Carbon Systems

BLANK PAGE

Part II. Ternary Systems

Volume I.	Ta-Hf-C System
Volume II.	Ti-Ta-C System
Volume III.	Zr-Ta-C System
Volume IV.	Ti-Zr-C, Ti-Hf-C, and Zr-Hf-C Systems
Volume V.	Ti-Hf-B System
Volume VI.	Zr-Hf-B System
Volume VII.	Systems Ti-Si-C, Nb-Si-C, and W-Si-C
Volume VIII.	Ta-W-C System
Volume IX.	Zr-W-B System, Pseudo-Binary System TaB_2-HfB_2
Volume X.	Systems Zr-Si-C, Hf-Si-C, Zr-Si-B, and Hf-Si-B
Volume XI.	Systems Hf-Mo-B and Hf-W-B
Volume XII.	Ti-Zr-B System
Volume XIII.	Phase Diagrams of the Systems Ti-B-C, Zr-B-C, and Hf-B-C
Volume XIV.	The Hafnium-Iridium-Boron System
Volume XV.	Constitution of Niobium-Molybdenum-Carbon Alloys
Volume XVI.	The Vanadium-Niobium-Carbon System
Volume XVII.	Constitution of Ternary Ta-Mo-C Alloys

Part III. Special Experimental Techniques

Volume I.	High Temperature Differential Thermal Analysis
Volume II.	A Pirani-Furnace for the Precision Determination of the Melting Temperatures of Refractory Metallic Substances

Part IV. Thermochemical Calculations

Volume I.	Thermodynamic Properties of Group IV, V, and VI Binary Transition Metal Carbides
Volume II.	Thermodynamic Interpretation of Ternary Phase Diagrams
Volume III.	Computational Approaches to the Calculation of Ternary Phase Diagrams.

This technical report has been reviewed and is approved.

W. G. RAMKE
Chief, Ceramics and Graphite Branch
Metals and Ceramics Division
Air Force Materials Laboratory

ABSTRACT

The zirconium-silicon and hafnium-silicon binary systems have been investigated by means of Debye-Scherrer X-ray analysis, metallography, melting points, differential analysis techniques, and chemical analysis.

Both silicide systems contain a $D8_8$-type phase which is stabilized by trace impurities of oxygen and nitrogen.

The binary phases present are: Zr_4Si, Zr_2Si, Zr_3Si_2, Zr_5Si_4, α- and β-ZrSi, and $ZrSi_2$; in the hafnium system: Hf_2Si, Hf_3Si_2, Hf_5Si_4, HfSi, and $HfSi_2$. The ZrSi phase undergoes an allotropic transformation at 1550°C; the high temperature form is of the CrB type, while the low temperature crystal structure is of the FeB type.

Complete phase diagrams from 1100°C up to melting are given.

TABLE OF CONTENTS

LIST OF ILLUSTRATIONS

LIST OF ILLUSTRATIONS (cont'd)

LIST OF TABLES

I. INTRODUCTION AND SUMMARY

A. INTRODUCTION

In our continuing research in the phase equilibria of binary, ternary, and higher order refractory metals of the IVa, Va, and VIa groups with boron, silicon, and carbon, the systems Zr-Si and Hf-Si have been investigated.

In view of the recent crystal structural investigations, it is safe to say that all of the crystal structures occurring in the binary Zr-Si and Hf-Si systems have been elucidated; nonetheless, the data available describing the physical constitution of these two binary systems are based in one instance (Zr-Si) on older, as yet not completely confirmed investigations, and in the other case (Hf-Si) on a hypothetical model based on cursory experimental data and on analogies to the Zr-Si system.

More exact experimental data are necessary, not only on the Hf-Si system, but in particular in the clarification of the effects on the binary phase equilibria by the suspected ternary-stabilized Me_5Si_3-$D8_8$ phase.

B. SUMMARY

1. The Zirconium-Silicon System

The zirconium-silicon system contains six intermediate phases of which only one, Zr_3Si_2 melts congruently. None of the phases has a homogeneous range.

The Zr_5Si_3 (C, N, O)-$D8_8$ phase, is a strongly stabilized ternary and higher order phase which has a sizeable homogeneous range from about 35 to 41 At.% Si. This $D8_8$ phase tends to suppress the formation of the binary Zr_3Si_2 and Zr_5Si_4 phases and is always closely associated with the Zr_3Si_2 phase. β-zirconium takes less than 2 At.% Si into solid solution at the β-Zr-Zr_2Si eutectic temperature; this eutectic temperature is 1575 ± 5°C, and the eutectic point is at 9 ± 1 At.% Si.

The Zr_4Si phase forms in a slow peritectoid reaction at about 1500°C. The measured lattice parameters of this phase crystallizing in the Ti_3P structure type are: a = 12.64 Å; c = 5.448 Å.

The Zr_2Si phase melts peritectically at about 1950°C to Zr_3Si_2 and melt, although the D8 phase strongly masks this reaction. The lattice parameters measured for the Zr_2Si, C-16 type phase are: $a = 6.60_4$ Å; $c = 5.31_4$ Å.

The Zr_3Si_2 phase, which melts congruently at 2324 ± 25°C and crystallizes in the tetragonal, U_3Si_2-type structure, has lattice parameters of; $a = 7.09_1$ Å; $c = 3.69_7$ Å.

The Zr_5Si_4 phase, a recently characterized tetragonal structure, melts peritectically at 2310 ± 10°C to Zr_3Si_2 and a silicon-richer melt; the lattice parameters are: $a = 7.12_7$ Å; $c = 13.01$ Å.

ZrSi undergoes a structural transformation at 1550 ± 10°C. The high temperature β form has the orthorhombic CrB-type structure which melts peritectically at 2220 ± 10°C to Zr_5Si_4 and a silicon-rich melt. The lattice parameters are: $a = 3.75_2$, $b = 9.90_3$, and $c = 3.74_9$ Å. The low temperature form, having lattice parameters of $a = 6.99_3$, $b = 3.78_4$, and $c = 5.30_1$ Å, crystallizes in the FeB, B-27 type.

$ZrSi_2$, which has the orthorhombic C-49 crystal structure, melts peritectically to β-ZrSi and a silicon-rich melt at 1584 ± 5°C. Its lattice parameters are: $a = 3.69_7$, $b = 14.74$, and $c = 3.66_6$ Å.

Between $ZrSi_2$ and silicon there is a eutectic at 90.0 ± 0.5 At.% Si; the eutectic temperature is 1353 ± 5°C.

Table 1 shows the isothermal reactions in the Zr-Si system, while Figure 1 shows the Zr-Si phase diagram based on the results of this investigation.

Table 1. Isothermal Reactions in the Zirconium-Silicon Binary System

Temperature °C	Reaction	Composition of the Equilibrium Phases, At.%Si			Type of Reaction
1876	$L \rightleftarrows \beta\text{-Zr}$	0	0	-	Melting Point of β-Zr
1575	$L \rightleftarrows \beta\text{-Zr} + Zr_2Si$	9	0.6	33.3	Eutectic Reaction
1500	$Zr_4Si \rightleftarrows \beta\text{-Zr} + Zr_2Si$	~20	<0.6	33.3	Peritectoid Reaction
1950	$L + Zr_3Si_2 \rightleftarrows Zr_2Si$	~23	40	33.3	Peritectic Reaction
2325	$L \rightleftarrows Zr_3Si_2$	40	40	-	Congruent Melting
2310	$L + Zr_3Si_2 \rightleftarrows Zr_5Si_4$	~46	40	44.4	Peritectic Reaction
2220	$L + Zr_5Si_4 \rightleftarrows \beta\text{-ZrSi}$	~50.5	44.4	50	Peritectic Reaction
1550	$\beta\text{-ZrSi} \rightleftarrows \alpha\text{-ZrSi}$	50	50	-	Allotropic Transform.
1584	$L + \beta\text{-ZrSi} \rightleftarrows ZrSi_2$	~70.5	50	66.7	Peritectic Reaction
1353	$L \rightleftarrows ZrSi_2 + Si$	90	66.7	~100	Eutectic Reaction
1430	$L \rightleftarrows Si$	100	100	-	Melting Point of Si

2. The Hafnium-Silicon System

The hafnium-silicon system contains five intermediate phases of which only Hf_3Si_2 is congruent melting. None of the phases show any appreciable homogeneous range.

The Hf_5Si_3 (C, N, O)-$D8_8$ compound is a ternary or higher order stabilized phase which is able to be disposed of, in some instances, by arc melting purification. It is always closely associated with the Hf_3Si_2 phase, tends to suppress the formation of the true binary phases Hf_3Si_2 and Hf_5Si_4, and has a homogeneous range from about 35 to 41 At.% Si.

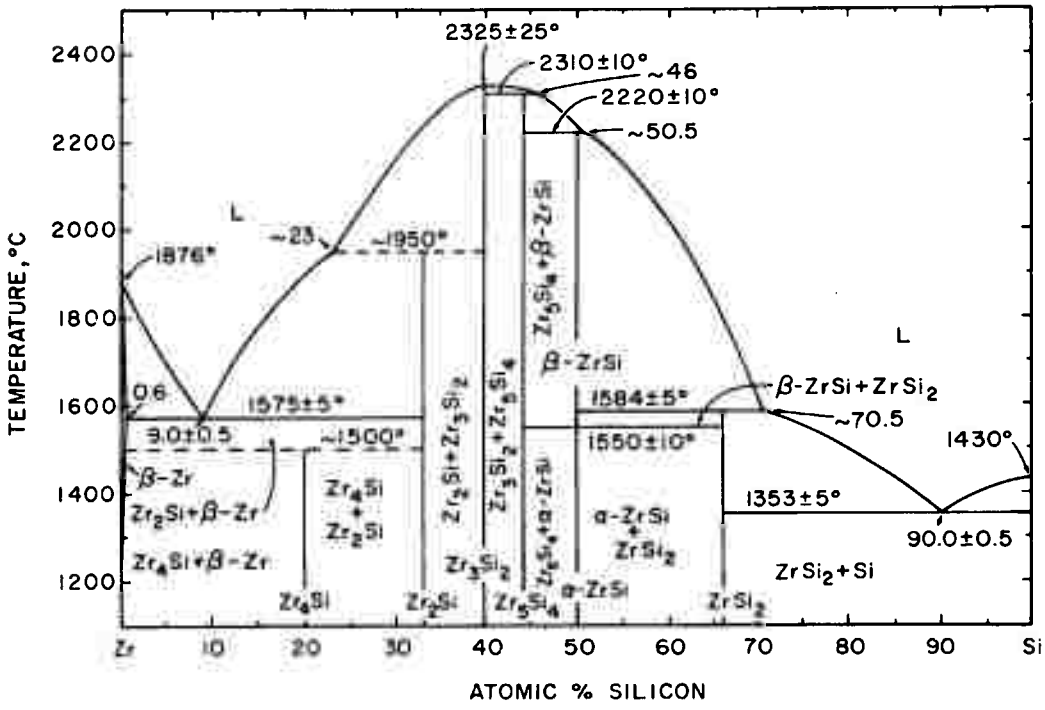

Figure 1. The Zirconium-Silicon System

β-Hf takes less than 1 At.% Si into solid solution at the β-Hf-Hf_2Si eutectic temperature; this eutectic temperature is 1831 ± 5°C, and the eutectic point is located at 12 ± 1.0 At.% Si.

An uncertain peritectoid reaction isotherm at about 1770°C, resulting from the α-β transformation of hafnium, is indicated to occur in the binary system.

Hf_2Si melts peritectically at 2083 ± 12°C into a hafnium-richer melt and Hf_3Si_2. The lattice parameters of the Hf_2Si phase which crystallizes in the tetragonal, C-16 structure are: a = 6.54$_7$ Å and c = 5.19$_0$ Å.

The Hf_3Si_2 phase melts congruently at 2480 ± 20°C; this high melting phase crystallizes in the tetragonal, U_3Si_2-type structure and has lattice parameters of: $a = 6.98_2$ Å, $c = 3.66_3$ Å.

The Hf_5Si_4 compound, which crystallizes in the Zr_5Si_4 tetragonal crystal structure, has lattice constants of $a = 7.02_3$ Å and $c = 12.88_2$ Å and melts peritectically to Hf_3Si_2 and a silicon-rich melt at 2320 ± 15°C.

At 2142 ± 15°C the HfSi phase, which unlike its Zr-Si homologue, does not undergo a crystal structural transformation, melts peritectically to Hf_5Si_4 and a silicon-richer melt. The lattice parameters of this phase with the FeB-type structure are: $a = 6.87_7$, $b = 3.77_0$, and $c = 5.22_9$ Å.

The silicon-richest phase, $HfSi_2$, decomposes peritectically at 1543 ± 8°C into a silicon-richer melt and HfSi. $HfSi_2$, which also has a negligible homogeneous range, solidifies in the $ZrSi_2$-C49, orthorhombic structure and has the following lattice parameters: $a = 3.67_4$, $b = 14.56$, and $c = 3.63_1$ Å.

Between $HfSi_2$ and silicon there exists a eutectic at 91.5 ± 1.0 At.% Si whose isothermal temperature is 1330 ± 8°C.

Table 2 shows the isothermal reactions occurring in the binary Hf-Si system, and Figure 2 depicts the Hf-Si phase diagram constructed from results of this investigation.

Table 2. Isothermal Reactions in the Hafnium-Silicon Binary System

Temperature °C	Reaction	Composition of the Equilibrium Phases, At.%Si			Type of Reaction
2218	$L \rightleftarrows \beta\text{-Hf}$	0	0	-	Melting Point of β-Hf
1831	$L \rightleftarrows \beta\text{-Hf} + Hf_2Si$	12	<1	33.3	Eutectic Reaction
~1770	$\alpha\text{-Hf} \rightleftarrows \beta\text{-Hf} + Hf_2Si$	<1	<1	33.3	Peritectoid Reaction
2083	$L + Hf_3Si_2 \rightleftarrows Hf_2Si$	~27	40	33.3	Peritectic Reaction
2480	$L \rightleftarrows Hf_3Si_2$	40	40	-	Congruent Melting
2320	$L + Hf_3Si_2 \rightleftarrows Hf_5Si_4$	~46.5	40	44.4	Peritectic Reaction
2142	$L + Hf_5Si_4 \rightleftarrows HfSi$	~51.5	44.4	50	Peritectic Reaction
1543	$L + HfSi \rightleftarrows HfSi_2$	~69	50	66.7	Peritectic Reaction
1330	$L \rightleftarrows HfSi_2 + Si$	91.5	66.6	~100	Eutectic Reaction
1430	$L \rightleftarrows Si$	100	100	-	Melting Point of Si

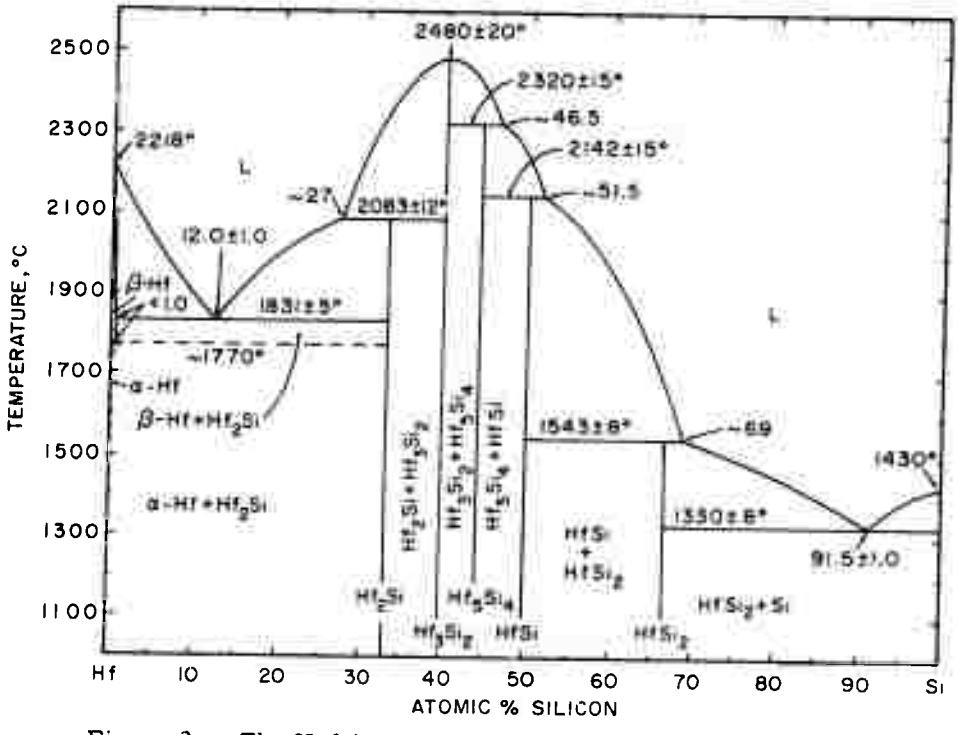

Figure 2. The Hafnium-Silicon System

II. LITERATURE REVIEW

A. THE ZIRCONIUM-SILICON SYSTEM

There have been a great number of crystal structural investigations in the zirconium-silicon system starting with the determination of the structure of $ZrSi_2$ by Seyfarth[1] in 1928. Not only are there a large number of phases and crystal structures, but also, the elucidation of the phases in the central portion of the system has been hampered considerably by the presence of an impurity phase stabilized by minute quantities of carbon, nitrogen, oxygen, and boron.

Naray-Szabo[2], Brauer[3, 4], Cotter et al.[5], and Nowtony[6] have also done confirmation and refinement work on the crystal structure of $ZrSi_2$. $ZrSi_2$ has an orthorhombic C-49 type structure. H. Nowotny et al.[7], P. Pietrokowsky[8], and L. Brewer[9] have all determined that Zr_2Si has the tetragonal, $CuAl_2$-type structure.

An extensive investigation of the Zr-Si system has been made by C.E. Lundin, D.J. McPherson, and M. Hansen[10]. These authors have found the following phases: Zr_4Si, Zr_2Si, Zr_3Si_2, Zr_4Si_3, Zr_6Si_5 ZrSi, and $ZrSi_2$. The phase diagram presented shows that Zr_4Si decomposes peritectically into liquid and Zr_2Si at 1630°C; Zr_2Si melts peritectically to liquid and Zr_3Si_2 at 2110°C, and Zr_3Si_2 also melts peritectically to Zr_4Si_3 and liquid at 2210°; Zr_4Si_3 is also said to melt peritectically at 2225°C to Zr_6Si_5 and liquid. Zr_6Si_5 is the only compound in the Zr-Si system which melts with a maximum; its melting point is 2250°C. ZrSi decomposes peritectically at 2095°C, and $ZrSi_2$ also melts peritectically at 1520°C. There is eutectic between β-Zr and Zr_4Si at 8.8 At.% Si at 1610°C; a second eutectic between $ZrSi_2$ and silicon is present at 90.0 At.% Si and 1355°C.

Nowotny and co-workers[7] in a later investigations, found no evidence of the Zr_6Si_5, Zr_4Si_3 and Zr_3Si_2 phases, but identified a Zr_5Si_3 phase with the hexagonal, $D8_8$ structure; the hexagonal indexing of ZrSi reported by Lundin et al.[10] was not confirmed. Nowotny et al.[6] later showed that ZrSi has the FeB, B-27 type structure.

Kieffer, Benesovsky, and Machenschalk[11] investigated the zirconium silicon system by means of melting point determinations, metallography, and X-ray analysis; they constructed a temporary constitution diagram containing the phases Zr_2Si, Zr_5Si_3, ZrSi, and $ZrSi_2$ which was in partial agreement with Lundin's[10] findings.

In renewed investigations of the Zr-Si system, with and without carbon additions, H. Nowotny and co-workers[12], as well as L. Brewer[13], were able to show that the binary phase previously denoted as Zr_5Si_3 is in

reality a ternary, $D8_8$ phase, Zr_5Si_3 (C), stabilized by carbon, oxygen, nitrogen, and boron. Furthermore, Brewer and Krikorian[13] state that the phase designated by C. Lundin[10] as Zr_3Si_2 corresponds to the Zr_5Si_3 (C) phase, and the Zr_4Si_3 is the Zr_3Si_2 phase which, after Pietrokowsky[14] has the U_3Si_2 type structure. C.H. Dauben[15] later also reported that Zr_3Si_2 was isostructural with U_3Si_2. H. Nowotny[12] further confirmed the existence of the Zr_6Si_5 phase[10] and designated it U-II because of its unknown structure and inexact composition; by the same token, another phase which seemed to be at about 40 At.% silicon was designated U-I.

In 1961 Nowotny and co-workers[16], in conjunction with work on the Zr-Si-Al system, were able to show that the U-II phase (Zr_6Si_5) was a CrB-structure-type monosilicide which always occurs at zirconium concentrations of somewhat less than 50 At.% Si, i.e. $Zr_{\sim 6}Si_{\sim 5}$. The authors were further able to confirm the findings of Brewer[13] and Dauben[15] that Zr_3Si_2 is isostructural with U_3Si_2; this Zr_3Si_2 phase is however; not the previously described[12] U-I phase. This U-I phase[12, 17] has a σ-similar structure and is isostructural with other, at that time unknown, phases in the Ti-Si and Hf-Si systems.

K. Schubert and co-workers[18, 19] have confirmed the existence of the Zr_4Si phase reported by Lundin[10], Knapton[20], Brewer[13], and Farkas[21], and further determined that this phase crystallizes in the tetragonal Ti_3P-type structure. Farkas[21] et al. have reported that the Zr_4Si phase is formed in a peritectoid reaction from β-Zr and Zr_2Si in a very slow reaction. Schubert[19] further states that the actual composition of this phase is probably somewhat zirconium-richer, i.e., Zr_4Si, than its structural formula, Zr_3Si, indicates.

In a recent piece of work, Schubert[22], in working with single crystals of the phase occurring in the region of 40-45 At.% Si (the previously designated U-I phase[12] has shown that this phase crystallizes in a tetragonal structure belonging to the space group D_4^4-$P4_12_12$ and is given the formula Zr_5Si_4 (44.4 At.% Si). In a later publication, Russian authors[23] have confirmed the structure of Zr_5Si_4.

The solubility of silicon in zirconium was determined by C. Lundin and co-workers[10]: α-zirconium dissolves a maximum of approximately 0.3 At.% Si whereas β-zirconium dissolves about 0.6 At.% Si at the eutectic temperature.

A constitution diagram (Figure 3) of the Zr-Si system, taken from Hartstoffe[24], shows the basic diagram of C. Lundin et al.[10] modified with some of the more recent findings; the new Zr_5Si_4 phase[22,23], as well as Schubert's[18,19], Zr_3Si phase are not depicted. Table 3 contains the established phases and crystal structures of the Zr-Si intermediate phases.

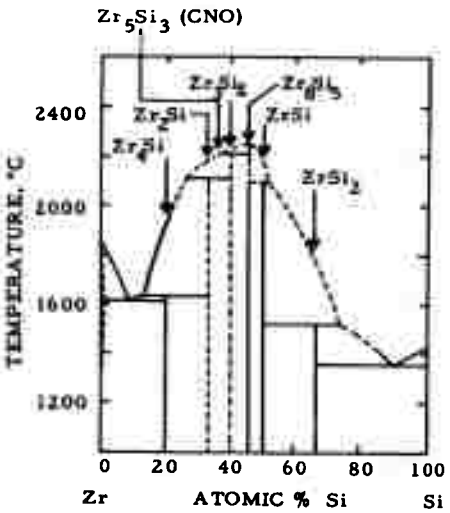

Figure 3. Zr-Si Constitution Diagram.
(C.E. Lundin, D.J. McPherson, and M. Hansen, 1953 — Modified by R. Kieffer[24], 1963).

Table 3. Lattice Parameters and Crystal Structures of Intermediate Zr-Si Compounds

Phase	Crystal Structure	Lattice Parameters in Å Angstrom	Literature
$ZrSi_2$	orthorhombic C49 type	a = 3.72 b = 14.76 c = 3.67	6
ZrSi	orthorhombic B-27 (FeB type)	a = 6.98 b = 3.78_6 c = 5.30_2	6
$Zr_{\sim 6}Si_{\sim 5}$	orthorhombic B_f (CrB-type)	a = 3.76_2 b = 9.91_2 c = 3.75_3	16
Zr_5Si_4	tetragonal D_4^4-$P4_12_12$	a = 7.122_5 c = 13.000	22
Zr_3Si_2	tetragonal (U_3Si_2 type)	a = 7.082 c = 3.715	13, 15, 16
Zr_2Si	tetragonal C-16 ($CuAl_2$-type)	a = 6.6120 c = 5.45	8
Zr_3Si (Zr_4Si)	tetragonal DO_e (Ti_3P-type)	a = 11.01 c = 5.45	18, 19

B. THE HAFNIUM-SILICON SYSTEM

The hafnium-silicon system has not yet been completely investigated, nor has a fully documented phase diagram been established, although probably all of the phases and crystal structures occurring in the Hf-Si system have been characterized. B. Post, F. Glaser, and D. Moskowitz[25] found two silicides, $HfSi_2$ and HfSi. $HfSi_2$ has an orthorhombic unit cell: Smith and Bailey[26] as well as Cotter et al.[5] have found that $HfSi_2$ is isostructural with the analogous zirconium silicide. By analogy[10], B. Post, et al.[25] stated that HfSi crystallizes in a hexagonal structure. It has subsequently been shown, however, by H. Nowotny and co-workers[27] that HfSi has an orthorhombic-FeB type structure. H. Nowotny[27] also prepared and identified the compound Hf_2Si. This compound has the $CuAl_2$-type structure and is isostructural with the zirconium silicon compound. H. Nowotny[26] found traces of a possible Hf_4Si phase, but could not identify the suspected compound more closely. The compound Hf_5Si_3 (C, N, O) has also been found[27] and characterized as having the $D8_8$-Mn_5Si_3 structure. In strong analogy to the Zr_5Si_3 (C, N, O) phase, it is suspected[27, 28] that the $D8_8$ phase is really a stabilized ternary phase and would not be found in the true binary system.

In 1961, H. Nowotny and co-workers[16] discovered two more phases in the Hf-Si system; one of these, Hf_3Si_2 has the tetragonal U_3Si_2 structure while the other phase, lying near 43 At.% Si, was described as having a σ-type similar structure; this phase is isostructural with the other, at that time unknown, phases in the Ti-Si and Zr-Si systems.

Nowotny, Braun, and Benesovsky[29] presented a hypothetical phase diagram of the hafnium-silicon system based on melting point determinations and analogies with the Zr-Si system. This temporary diagram, (Figure 4), does not include the more recent findings concerning the probable absence of the Hf_5Si_3 phase, the presence of the Hf_3Si_2, and the existence of the σ-similar phase.

Recently, K. Schubert et al.[19, 22] were able to show that the unidentified phase[16] lying near 43 At.% Si is Hf_5Si_4 which has a tetragonal

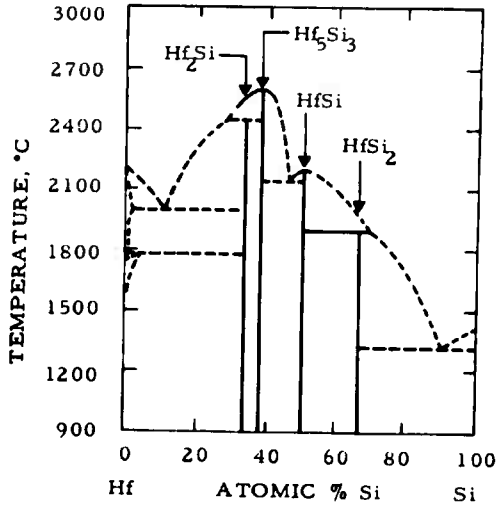

Figure 4. Hf-Si: Hypothetical Constitution Diagram.
(H. Nowotny, H. Braun, and F. Benesovsky, 1960).

unit cell and is isostructural to the Zr_5Si_4 phase. These authors further stated that no evidence was found for the existence of a "Hf_4Si" compound.

Table 4 gives the crystal structures and lattice parameters of the known Hf-Si phases.

Table 4. Lattice Parameters and Crystal Structures of Intermediate Hf-Si Compounds

Phase	Crystal Structure	Lattice Parameters in Angstroms	Literature
Hf_2Si	tetragonal $CuAl_2$-type (C-16)	a = 6.48 c = 5.21	27
Hf_5Si_3(C,N,O,B)	hexagonal Mn_5Si_3 type ($D8_8$)	a = 7.89_0 c = 5.55_8	27
Hf_3Si_2	tetragonal U_3Si_2 type	a = 7.00_0 c = 3.67_1	16
Hf_5Si_4	tetragonal, Zr_5Si_4 type	a = 7.03_9 c = 12.82_6	19, 22
HfSi	orthorhombic FeB type (B-27)	a = 6.85_5 b = 3.75_3 c = 5.19_1	27
$HfSi_2$	orthorhombic $ZrSi_2$ type	a = 3.677 b = 14.550 c = 3.649	26

III. EXPERIMENTAL PROCEDURES

A. STARTING MATERIALS

Elemental as well as pre-pared disilicide powders were used as starting materials for the alloys investigated.

The zirconium metal powder used was obtained from the Wah Chang Corporation, Albany, Oregon and had the following main impurities (in ppm): C-40, Nb-<100, Fe-315, Hf-67, N-34, O-830, Si-<40, Ta-<200, Ti-<20, and W-<25. The lattice parameters of this starting material were a = 3.232 Å and c = 5.149 Å. The metal powder was sized between 74 and 44 micrometers. Spectrographic analysis performed at the Aerojet Metals and Plastics Chemical Testing Laboratory yielded the following results (in ppm): Si-10, Fe-20, Ta-not detected, and Hf-500.

The hafnium metal powder was also supplied by the Wah Chang Corporation, Albany, Oregon; the vendor's analysis was (in ppm): Al-97, C-40, Nb-<100, Fe-96, H-90, N-130, O-850, Si-<40, Ta-200, and W-<25. This hafnium contained 2.5% by weight of zirconium. The average particle size was <44 micrometers; lattice parameters of a = 3.19_5 Å and c = 5.05_6 Å were obtained from a powder diffraction pattern taken with Cu-K_α radiation.

The silicon used was supplied by the Var-Lac-Oid Chemical Company, New York and had the following vendor's analysis (in ppm): Fe-500, Al-100, Ca-200, Ti-10, Cr-50, Mn-30, Cu-10, and Ni-trace. The particles were sized smaller than 44 microns. The Aerojet Metals and Plastics Chemical Testing Laboratory's spectrographic analysis of these materials was (in ppm): C-80, Cr-100, Ni-<10, Cu-800, Al-1000, Fe-250, Ti-400, Mg-<10, B-10, and Ca-500. The lattice parameter of this starting material was 5.429_7 Å.

Both the zirconium and hafnium disilicides were prepared in the same manner, taking precautions and steps to avoid any contamination by oxygen, nitrogen, and carbon; the master alloys were arc melted to remove as much contaminate oxygen as possible. Owing to the strong exothermic

reaction between the metals and the silicon, the alloys were prepared in two steps in the following way. A silicon-rich mixture, containing about 80 At.% Si with the balance zirconium or hafnium, respectively, was cold pressed into small 3/4" dia. slugs and arc melted well on both sides under an atmosphere of reactor grade helium in a nonconsumable tungsten arc melting furnace. The yellow deposit of SiO was removed from the surface of the samples and the furnace hearth. After crushing lightly by hand, the alloy was rough ground in a carbide ball mill to approximately 200 micrometer size under carbon tetrachloride, cold dried under vacuum, and acid leached to remove iron, cobalt, and nickel from ball milling, acetone washed, cold vacuum dried, and mixed with the respective metals to yield a disilicide composition. The cold pressing, arc melting, ball milling, leaching, and drying procedures were repeated with the final disilicide alloy powder. The powders,which were sized smaller than 88 micrometers,were analyzed for their silicon content. The zirconium disilicide contained 36.47 Wt.% Si (65.1 At.%) and the hafnium disilicide 22.35 Wt.% Si (64.7 At.% Si). Debye-Scherrer X-ray photographs of these materials showed, in the case of $ZrSi_2$, the C-49 orthorhombic disilicide pattern with small amounts of ZrSi in both the FeB type and CrB type structures. The hafnium alloy contained a small quantity of HfSi (FeB type) next to the major constituent, $HfSi_2$ (C-49 type).

B. ALLOY PREPARATION AND HEAT TREATMENT

1. Melting Point, Differential Thermal Analysis, and Derivative Thermal Analysis Samples

The melting point samples for the two silicide systems were prepared from the respective disilicide and metal or silicon elemental powders as needed. Some of the samples were hot pressed in graphite dies and exceedingly well surface cleaned to remove all chances of carbon contamination, but most of the melting point alloys were made by cold pressing the mixtures in a special retractable pin, reduced-center-area die arrangement yielding a 34 mm long sample such as shown in Figure 5.

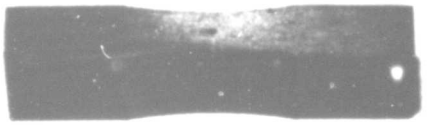

Figure 5. Typical Cold Pressed Melting Point Sample Showing Reduced Center Portion and 0.6 mm Black Body Hole.

The green compacts were given a strengthening heat treatment for 2 hours at 1200°C under static, reactor-grade helium.

The cylindrical, hot pressed melting point slugs were reduced in the center and drilled with a 1.0 mm hole for black body hole temperature measurement.

The differential thermal analysis samples were made in two ways. Some samples were hot pressed from elemental and disilicide powders in graphite dies with a black body hole in the sample and surface cleaned well; other samples were cold pressed from elemental powders and arc melted when the effect of oxygen and nitrogen contamination was deemed especially critical.

2. Solid State and Arc Melted Samples

After the melting point experiments, portions of the melted zones of these samples were ground for X-ray powder photograph analysis and the remaining piece of the sample arc melted under helium for metallographic examination and subsequent heat treating at 1300°, 1500°, 1600°, 1800°, and 2000° (depending on composition) under static helium for 20-70 hours in a tungsten mesh,Brew-furnace. The top of the tantalum can containing the samples to be heat treated was covered with zirconium sponge to act as a getter for any possible trace amounts of oxygen and nitrogen.

In no case did the samples show discoloration from contamination with gaseous metalloids, and no sintering or melting effect of the samples with the tantalum container was observed.

C. DETERMINATION OF MELTING TEMPERATURES

Melting points of the alloys in the two binary systems were determined by direct resistance heating of the samples. Observation of melting was conducted using the Pirani-hole method. The special melting point furnace and the Pirani-technique have been previously described[30] in this series of reports.

The temperature measurements were carried out with a disappearing-filament type micropyrometer which was calibrated against a certified, standard lamp from the National Bureau of Standards. The temperature correction for the absorption in the quartz furnace window, as well as that for deviation due to non-black body conditions have been amply described and validated in a previous report[30].

The melting point experiments were conducted under high purity helium at 2-1/4 atmospheres pressure to prevent undue vaporization of silicon.

Some difficulty was encountered in the heating of the silicon-rich alloys. At normal temperatures, these materials have a very low

electrical conductance, and it was difficult to initially heat the samples using the direct resistance method. This difficulty was overcome in some cases by rubbing a small amount of molybdenum powder on the ends of the sample to provide a better contact between the sample and the tungsten insulating plate in the melting point furnace. The melting of the sample occurred in the center of the sample in the reduced area at the black body hole, and no contamination of the molten portion of the sample was possible. In some cases, primarily in the region of the disilicide-silicon eutectic (Zr-Si system) no melting point measurements using the Pirani technique were possible, and the melting points were determined using the indirect heating of the differential thermal analysis method.

D. DIFFERENTIAL AND DERIVATIVE THERMOANALYTICAL STUDIES

The differential thermal analysis methods and techniques used with the specially designed and constructed equipment in use in this laboratory have been extensively described and documented in an earlier report[31] of this series.

It must be noted, however, that special precautions and techniques were necessary to reduce or prevent reaction and contamination of the silicide samples with graphite, yielding erroneous data for the binary silicide systems. In those instances where the experimental data desired lay considerably below the melting point of zirconium, a thin zirconium shielding was placed between the silicide sample and the graphite DTA sample holder to prevent interaction between the silicide and graphite. The slight carburization of the zirconium shield occurs very slowly over a range of temperatures up to the melting point of the Zr-ZrC eutectic. This diffusion process was never actually observed in the thermograms due to the small amount of shielding used in comparison to the size of the silicide sample. The zirconium shielding could not, of course, be used in those temperature ranges above the melting point the zirconium carbide eutectic, or for that matter, above those melt-solid isotherms lying between the zirconium silicide composition of the sample used and zirconium metal, for isothermal reactions resulting from silicide reaction

with the zirconium shield would be recorded, disguising possible reactions in the sample itself.

Since the diffusion of graphite into the bulk of a silicide sample proceeds at a somewhat slow rate, especially without the presence of melt, a one-shot technique was employed where the silicide sample was in direct contact with graphite[31] for those samples which were investigated above the melting point of zirconium. Each of the high melting silicide samples was run up into the higher temperature (>1200°C) ranges but once and the results recorded. In this manner contamination with graphite in the bulk of the sample was avoided.

Derivative thermal analysis experiments using the Pirani melting point furnace with cold pressed and heat treated samples avoid the container contamination (graphite-silicide interaction) present with the use of the normal differential thermal analysis equipment.

The image of the black-body hole of the sample, which is clamped between two water cooled copper electrodes, is focused onto a photocell whose output is amplified and differentiated with respect to time. The time derivative of the temperature is then plotted against the amplified output (temperature) by means of a X-Y recorder. The output of the photodiode is compared with the output of a ramp generator (temperature command input) producing an error signal which is amplified and used to control the power delivered to sample for time-controlled heating and cooling rates[32].

E. METALLOGRAPHY

Metallographic studies were made of the melted portions of melting point samples as well as of arc melted specimens. Special metallographic samples were prepared by arc melting the elemental constituents in the desired proportions directly in the tungsten button arc furnace under high purity helium in spite of the occurrence of the heavy exothermic reaction upon alloying. In this manner, the most protection against sample contamination by oxygen and nitrogen was achieved. The samples were prepared by mounting

the alloys in an electrically conductive mixture of diallyl-phtalate-lucite copper base mounting material. The samples were roughly ground on varying grit sizes of silicon carbide paper; the final polishing was performed on a microcloth using a suspension of 0.05 micrometer alumina in Murakami's solution.

The silicide samples were all electroetched in a 2% NaOH aqueous solution; the silicon-rich alloys were then dip etched in an aqueous aqua regia-hydrofluoric acid solution (9 parts H_2O - 1 part acid mixture) (60% HCl- 20% HNO_3-20% HF).

Etchants which would selectively attack only one or more of the many silicide phases could not be discovered. Both oxalic acid and NaOH produced only gradually varying color changes in the silicides depending on metal content. The majority of the silicide phases were differentiated among themselves by careful comparison of the metallographic specimen with the corresponding X-ray film. Some of the silicides showed a considerable amount of intragranular cracking produced upon cooling; this in itself was sufficient for identification in many instances.

F. X-RAY ANALYSIS

Debye-Scherrer X-ray photographs were made of all samples in the Zr-Si and Hf-Si samples after solid state heat treatment, melting point experiments, DTA studies, and arc melting. Because of the complicated X-ray patterns offered by the many silicide compounds, chromium K_α radiation was used exclusively to spread out the diffraction lines.

Due to the rapid crystal structural transformation which occurs in both the hafnium and zirconium metals, the high temperature β-form of the metals was never observed in the X-ray patterns of samples which were at high temperatures.

The structures of the zirconium and hafnium silicides are known, and no difficulty was encountered in indexing and calculating lattice parameters

of these phases. Films of good quality were obtained of β-ZrSi, the CrB type, high temperature modification.

G. CHEMICAL ANALYSIS*

Chemical and spectrographic analyses were performed on some of the starting materials to check the vendor's analyses. In addition, the pre-prepared master silicides were analyzed for their silicon contents. Random analyses were made of the silicide alloys used in the experiments. The silicon loss, mostly attributed to arc melting, was not greater than 3 At.% Si in any case. The interstitial impurities of some of the starting metal powders were checked using a vacuum fusion technique in a platinum bath.

Silicon was determined by fusing the sample in a sodium hydroxide-sodium peroxide mixture, dissolving the melt in perchloric acid and volatilizing the silicon as Hf_2SiF_6 with a hydrofluoric-sulfuric acid mixture.

The spectrographic analyses showed that there was no major metallic impurity present in the starting materials which would seriously affect the high temperature equilibrium. The values of the interstitial contents (O, N, H) of the starting materials were somewhat higher than those indicated by the vendor; this discrepancy, however, is attributed to the time interval between Aerojet's and the vendor's analyses; the metal powders had sufficient time to adsorb both water and air.

IV. RESULTS

A. THE ZIRCONIUM-SILICON SYSTEM

The zirconium-silicon system, in comparison to the hafnium-silicon system, presented much greater difficulties in the interpretation and

*The chemical analyses were performed under the direction of W.E. Trahan in the Aerojet-General's Metals and Plastics Chemical Testing Laboratory.

documentation of the phase equilibria in the region from about 20 to 40 At.% silicon due to the presence of the ternary and higher order stabilized $D8_8$ phase; it is apparent that this Zr_5Si_3 (C, N, O) phase is considerably more stable in the zirconium system than in the hafnium system, although there seems to be little doubt that it is a trace impurity stabilized phase.

Lundin et al.[10] have reported that the silicon solubility in β-Zr is 0.6 At.% and the solubility in α-Zr, 0.3 At.%. An arc melted Zr-Si alloy, in this investigation, with 2 At.% Si (Figure 6) showed considerable amounts of the β-Zr-Zr_2Si eutectic on the grain boundaries indicating the silicon solubility in β-Zr is considerably less than 2 At.%. The solubility of silicon in α-zirconium was not specifically investigated, but the values of 0.3 At.% from Lundin[10] as well as 0.6 At.% for β-Zr were accepted and are so indicated in the phase diagram (Figure 22).

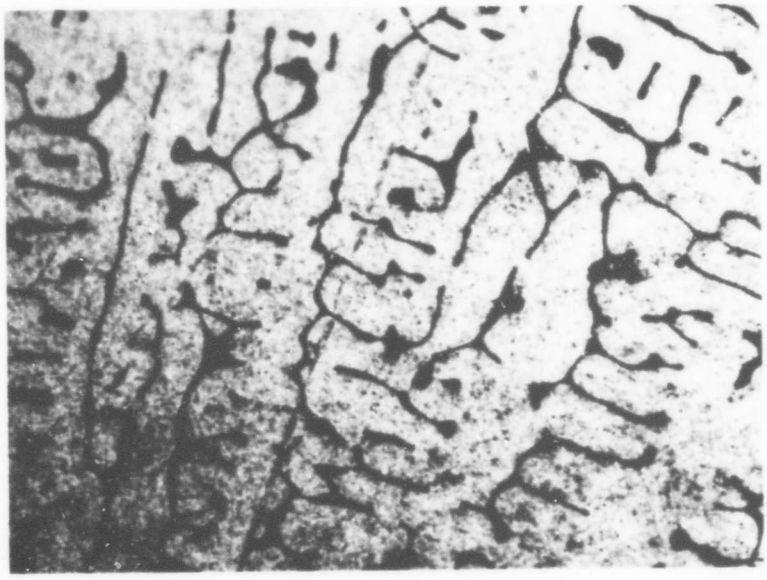

Figure 6. Zr-Si: An Arc Melted 98-2 Alloy X600

Primary β-Zr (Transformed) with β-Zr (Transformed)-Zr_2Si Eutectic (Not Resolved) on Grain Boundaries.

Measurements on fifteen Pirani melting point and four DTA specimens in the range of 3 to 25 At.% silicon indicated that the isothermal solidus temperature in this concentration range is 1575 + 5°C (Figures 7 and 21). A eutectic is formed between β- Zr and Zr_2Si; by metallographic means, the eutectic point was located at 9.0 ± 0.5 At.% Si which is in good accord with the findings of Lundin[10]. Figures 8, 9, and 10 depict the metallographic results of the arc melted alloys in this region.

Contrary to the findings of Lundin[10], no evidence for the peritectic formation of a Zr_4Si compound at 1630°C was observed. The melting points measured in this region by the Pirani method as well as by DTA were all grouped closely about the eutectic temperature of 1575°C. Metallographically, small amounts of the impurity $D8_8$ phase might have been taken for a Zr_4Si in the investigations by Lundin[10].

In this investigation,arc melted samples near 20 At.% Si, viewed metallographically, showed only the Zr_2Si phase, β-Zr and, at silicon-richer concentrations, some amount of the $D8_8$ phase as confirmed by examination of the Debye-Scherrer powder photographs.

The appearance of a Zr_4Si phase in practically pure form was observed after heat treating arc melted alloys which were quite close to the stoichiometric composition at 1500°C for 60 to 80 hours. The Debye-Scherrer pattern of a Zr-Si 80-20 alloy showed two phases, β-Zr and Zr_2Si present after arc melting, but after the long time heat treatment at 1500°C, an entirely different pattern, along with traces of β-Zr was present. The DTA experiments, on alloys near Zr_4Si however, were unable to detect any thermal arrests other than eutectic melting at 1575°C. Metallographic examination of the arc melted alloys after heat treatment showed that the eutectic structure formerly present in the arc melted specimens had changed to a completely annealed microstructure. Since phases existing in a relatively small silicon concentration region are quite insensitive to sharp color changes with the metallographic etchants used, the metallographic studies were not able to indicate a color difference between the Zr_4Si and Zr_2Si phases. The relative amounts of

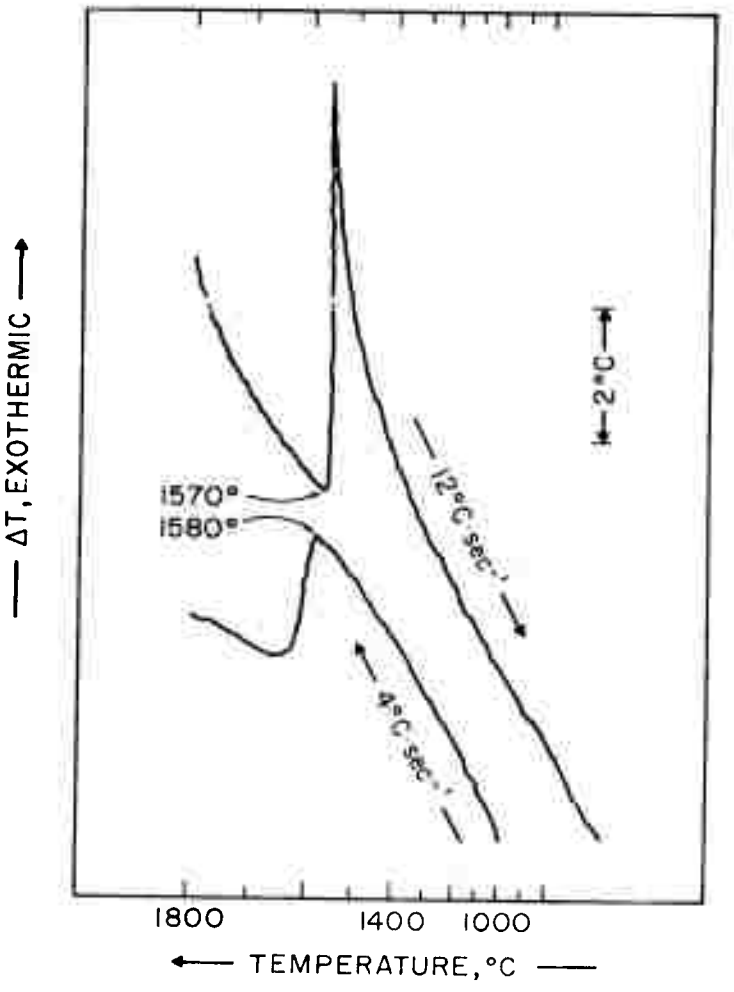

Figure 7. DTA Thermogram of a Zr-Si 92-8 Alloy Showing Eutectic Melting and Solidification.

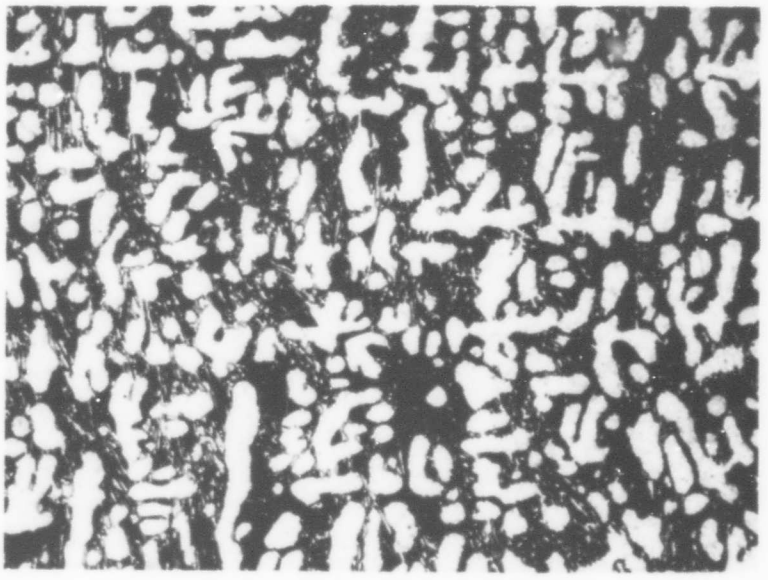

Figure 8. Zr-Si: An Arc Melted 93-7 Alloy. X520
Primary β-Zr in a β-Zr(Transformed)-Zr_2Si Eutectic Matrix.

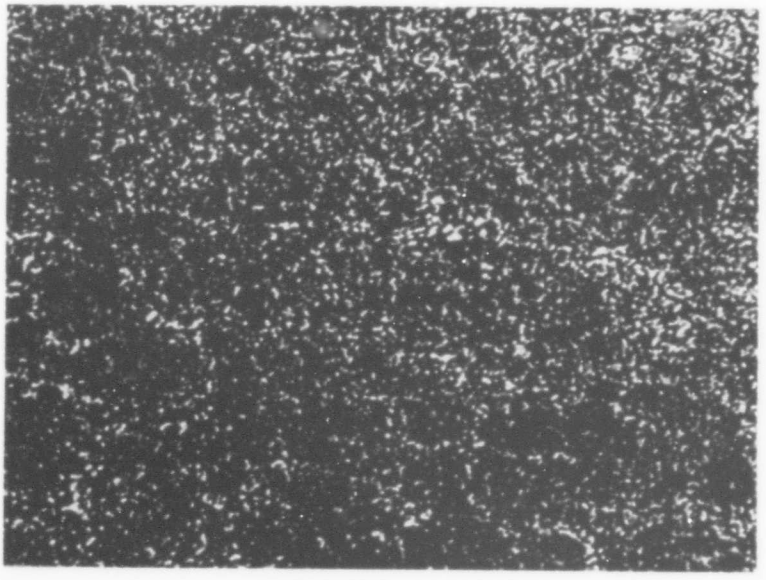

Figure 9. Zr-Si: An Arc Melted 90-10 Alloy (Eutectic Portion) X1000
Fine β-Zr(Transformed)-Zr_2Si Eutectic.

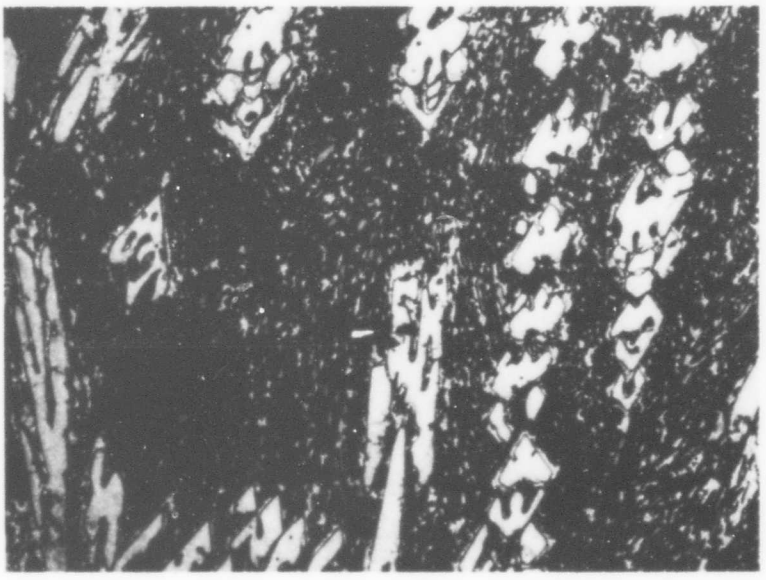

Figure 10. Zr-Si: An Arc Melted 85-15 Alloy. X520

Primary Zr_2Si in a β-Zr(Transformed)-Zr_2Si Eutectic Matrix.

the silicide and metal phase seemed to change inasmuch as the amount of silicide present in heat treated specimens was considerably more, while the amount of metal present was less than in the arc melted, eutectic containing sample. This observation, in conjunction with the fact that the Debye-Scherrer films showed the practically pure pattern of the Zr_4Si phase, indicated that most probably a peritectoid reaction in which Zr_4Si is formed from β-Zr and Zr_2Si had proceeded to completion. Figure 11 shows the microstructure of the ZrSi 80-20 annealed alloy containing the Zr_4Si phase.

Since the exact temperature of the peritectoid reaction could not be determined, it is indicated with uncertainty (Figure 22) at about 1500°C. These results are in substantial agreement with the findings of Farkas et al.[21] who also have indicated a peritectoid formation of Zr_4Si.

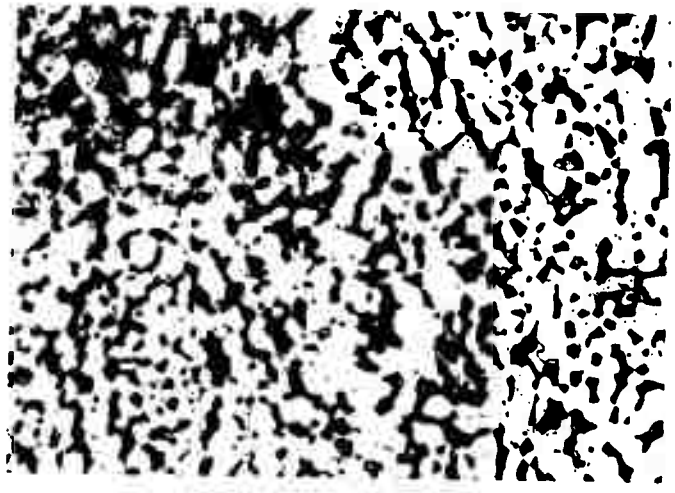

Figure 11. Zr-Si: An Arc Melted (80-20) Alloy Heat Treated 80 Hours at 1500°C. X100

Two Phased Alloy Consisting of Zr_4Si and β-Zr(Transformed).

An indexing of a powder photograph of Zr_4Si using the Ti_3P-type tetragonal unit cell as reported by Schubert et al.[18] was possible. However, the a spacing measured in this investigation differed substantially from that reported by Schubert[18] (see Table 3). The values measured were a = 12.64 Å and c = 5.448 Å.

As also reported by Schubert[19], the actual composition of the phase is quite close to Zr_4Si. Although the structural formula is Zr_3Si, the Zr_4Si phase apparently exists as a defect structure with voids in the silicon positions.

The investigation of the phase equilibria in the region between about 25 and 38 At.% silicon presents difficulties which are not able to be overcome by normal powder metallurgical means. Contrasting to the behavior of alloys in the same region in the Hf-Si system, the Zr-Si alloys were found

to contain considerable amounts of, and in most cases almost pure, $Zr_5Si_3(C,N,O)$-$D8_8$ phase. The $D8_8$ phase is much more easily stabilized by small quantities of carbon, oxygen, and nitrogen impurities in the Zr-Si system than in the hafnium system. The dominance of the $D8_8$ phase in the zirconium system is so strong that it completely disguises the peritectic melting isotherm of the Zr_2Si compound. Initial experimental Pirani melting point data indicated that the melting points (peritectic melting isotherm) for alloys with between 33 and 38 At.% Si were at an unusually high temperature of about 2345°C. Metallographic inspection as well as examination of the Debye-Scherrer powder diagrams of these melting point specimens showed them to contain the $D8_8$ phase almost exclusively. As also was the case with the Hf-Si alloys, the amounts and lattice parameters of the $D8_8$ phase in the various alloys whose temperature history was higher than about 1600°C showed a course completely independent of either silicon or zirconium content. The $D8_8$ phase, formed in the composition range of the Zr_3Si_2 compound was not able to be removed or substantially lessened by arc melting as is the case in the hafnium system. Nonetheless, it is quite apparent that the $D8_8$ phase found in the Zr-Si binary system, which incidentally formed in somewhat smaller quantities in samples which were not subjected to temperatures above 1600°C, is a ternary or higher order stabilized phase which is considerably more stable than its Hf-Si counterpart. The melting points measured in the vicinity of the Zr_2Si composition (~2345°C) obviously are the melting points of the Zr_5Si_3 (C, N, O)-$D8_8$ phase which definitely has a considerable homogeneous range from about 25 to 40 or more atomic percent silicon. These melting point measurements are not depicted in the diagram (Figure 21) showing the experimental data. Some metallographically examined specimens from this region showed a peritectic reaction taking place, but the reaction seen (Figure 12) is a ternary peritectic reaction involving the formation of Zr_2Si from the $D8_8$ phase and melt as also described by Schubert[22].

The decisions drawn from the peritectic reaction observed metallographically and supported by analogies between the remainder of the Zr-Si system and its sister Hf-Si system, where, in general, the incipient melting temperatures are somewhat higher, lead to the conclusion that the Zr_2Si phase must decompose peritectically at a temperature somewhere in the vicinity of 1950°C. This temperature, in the absence of adequate melting point data,

Figure 12. Zr-Si: An Arc Melted 77-23 Alloy. X500

Ternary Peritectic Reaction: Large Grains with White Centers (Primary $D8_8$ Phase) surrounded by Peritectic Walls of Hf_2Si in a β-Zr(Transformed)-Zr_2Si Rest Eutectic Matrix.

is indicated with uncertainty in the constructed phase diagram. It is not very probable, again in analogy to the Hf-Si system, that the melting point (2110°C[10] of Zr_2Si phase as was reported by Lundin[10], is higher than the melting temperature of Hf_2Si (2083°C, Figure 39).

A careful examination of X-ray powder photographs of arc melted and heat treated specimens containing Zr_2Si phase shows that there is no homogeneous range associated with this compound and it is essentially a line compound.

The only compound which melts with a maximum in the Zr-Si system is the Zr_3Si_2 compound at 2325 ± 25°C.

As with the analogous Hf_3Si_2 phase, the Zr_3Si_2 is always very strongly associated with the $D8_8$ impurity phase; in most instances, however, it is completely suppressed by the $D8_8$ phase. If the presence of the $D8_8$ phase is excluded, or for that matter, considered as being part of the Zr_3Si_2 phase, the interpretation of the phase equilibria in the center portion of the Zr-Si system can be more readily accomplished.

Figure 13 shows a two phased Hf_3Si_2-$D8_8$ structure indicating the validity of a maximum melting Zr_3Si_2 under exclusion of the $D8_8$ phase. The lattice parameter measurements of the Zr_3Si_2, using the tetragonal unit cell given by Schob[15], were determined as: $a = 7.09_1$ Å and $c = 3.69_7$ Å. There was no variance of the lattice parameters of the Zr_3Si_2 phase, within experimental measurement error, indicating the homogeneous range of this phase to be quite narrow.

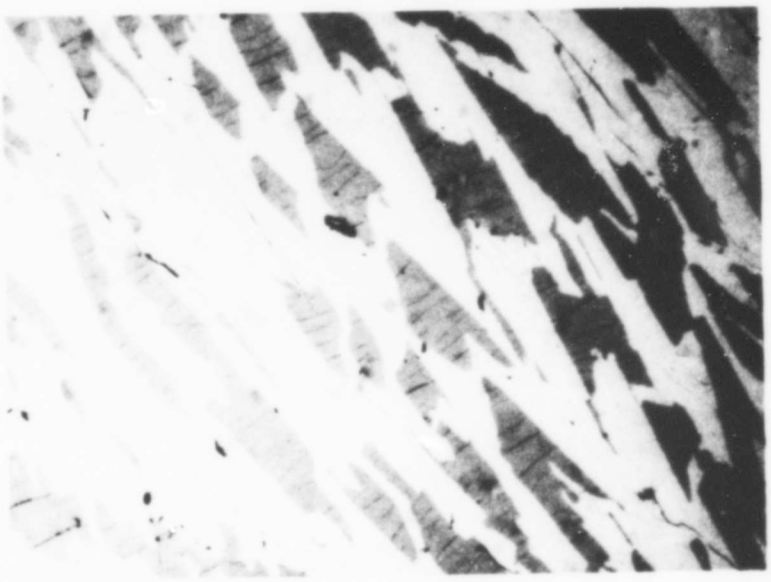

Figure 13. Zr-Si: An Arc Melted 60-40 Alloy. X520

Primary $D8_8$ phase (Dark with Cracks) in a Hf_3Si_2 Matrix.

Alloys in the range of about 41 to 44.5 At.% silicon melted at or quite close to 2310°C, the peritectic decomposition temperature of Zr_5Si_4. This compound melts to Zr_3Si_2 and a silicon-richer liquid.

The peritectic reaction was documented both metallographically (Figure 14) as well as by X-ray means, although in many instances the reaction was disguised by the presence of the $D8_8$ stabilized phase. In examining the X-ray films of arc melted, melting point, and heat treated specimens it was seen that the Zr_5Si_4, crystallizing in the tetragonal D_4^4-$P4_12_12$ structure characterized by Schubert[22] has a negligible homogeneous range. The lattice parameters were: $a = 7.12_7$ Å and $c = 13.01$ Å.

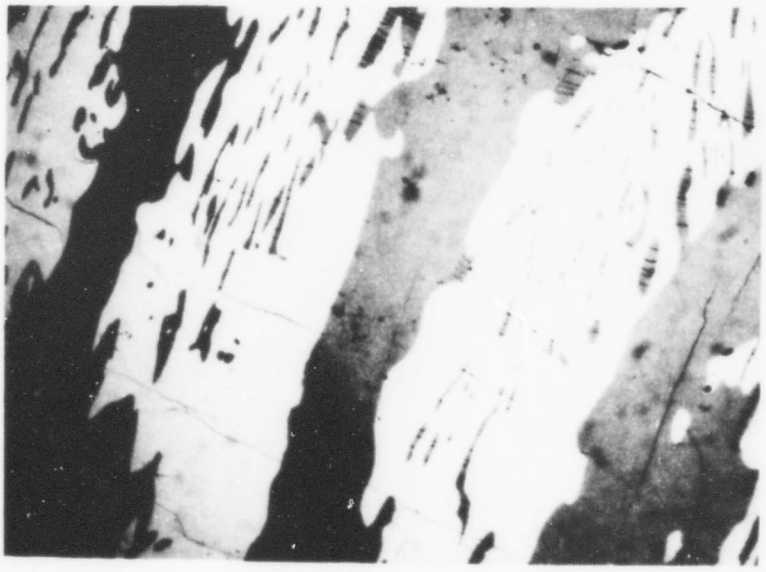

Figure 14. Zr-Si: An Arc Melted 57-43 Alloy. X400 (Polarized Light)

Primary Crystallized Zr_3Si_2 (Light Grains Containing Small Amounts of the Cracked $D8_8$ Phase) Surrounded by Peritectic Walls of Zr_5Si_4 (Peritectic Reaction Almost Completed)

The monoatomic compound ZrSi, which also melts peritectically at 2220 ± 10°C (Figure 15) into Zr_5Si_4 and a silicon-richer melt, was found to undergo a structural transformation at 1550 ± 5°C. The higher temperature form β-ZrSi, (Figures 21 and 22) has been referred to alternatively as Zr_6Si_5[16], U-II[12], and $ZrSi_{1-x}$[33]. This high temperature form, which crystallizes in the orthorhombic, CrB-type, is obtainable only by quite rapid quenching, such as in a button arc melter. A single phased Zr-Si 50-50 alloy which was arc melted showed only the ZrSi-CrB type structure with lattice parameters of $a = 3.75_2$ Å, $b = 9.90_3$ Å, and $c = 3.74_9$ Å. This same alloy, when heat treated at 1500°C was found to contain the orthorhombic FeB, B-27 type structure with lattice parameters of $a = 6.99_3$ Å, $b = 3.78_4$ Å, and $c = 5.30_1$ Å. The lattice parameters of both the α- and β-ZrSi showed virtually no change when observed in either two phased or single phased alloys heat treated at various temperatures. Both the high and low temperature forms have, therefore very restricted homogeneous ranges.

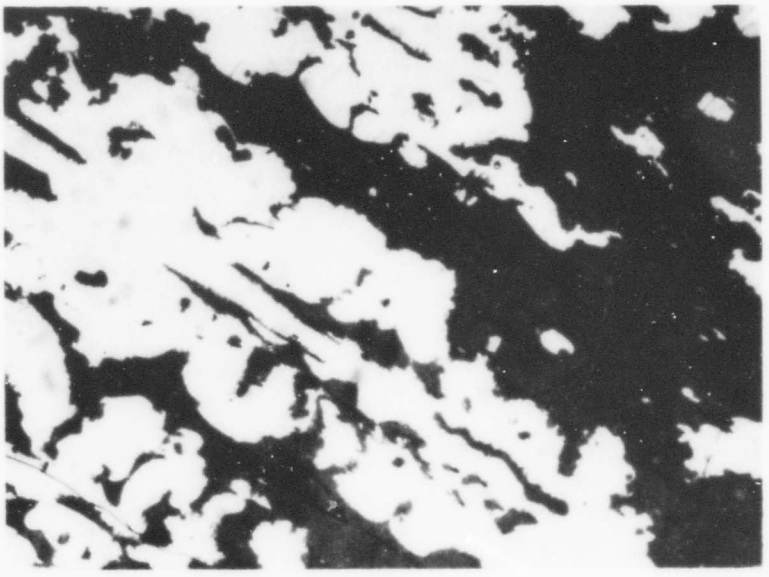

Figure 15. Zr-Si: An Arc Melted 52-48 Alloy. X250

Primary Crystallized Zr_5Si_4 (White Grain) Surrounded by Peritectic Walls of β-ZrSi Containing Rest Si-Rich Melt (Etch Pitted Dark Streaks).

Metallographically, no evidence of a transformation structure could be observed; however, DTA experiments run on samples in the range from 47.5 to 51.5 At.% all showed a sharp, exothermic peak on cooling and a similar endothermic thermal arrest on heating at about 1550°C. In alloys containing more than 50 At.% Si, the small amount of melt formed by the peritectic decomposition of $ZrSi_2$ causes an additional exothermal arrest to be superimposed on the transformation arrest (Figure 16). The sharpness of the thermal arrest attests to the rapidity of the transformation, and this, coupled with the fact that the transformation proceeds practically to completion as evidenced by X-ray results, is an explanation for the difficulty over the years in obtaining only small traces of the high temperature form. A publication by Schubert[22], who cites work by H. Nowotny, et al.[7, 16] gives reference to high and low temperature forms of ZrSi with the CrB and FeB structure types, but no details are given either in the Schubert work or in the older Nowotny works.

Seven Pirani melting point measurements and one DTA experiment document the peritectic decomposition temperature of $ZrSi_2$; the peritectic temperature of $ZrSi_2$ which melts to β-ZrSi and a silicon-richer melt is 1584 ± 5°C. Figure 17 shows a photomicrograph of the peritectic reaction occurring in the composition range about $ZrSi_2$. The lattice parameters were: $a = 3.69_7$, $b = 14.74$, and $c = 3.66_6$ Å.

Considerable difficulty was experienced in measuring melting points in the silicon richer-region beyond $ZrSi_2$ using the Pirani technique. The temperature dependent electrical resistivity of the semi-conductor silicon made it impossible to heat the melting point specimens by direct resistance; nonetheless, the melting point of the $ZrSi_2$-Si eutectic was determined by two DTA experiments (Figures 18 and 21). The eutectic temperature is 1353 ± 5°C, and the eutectic point, located by metallography, (Figures 19 and 20) lies at 90.0 ± 0.5 At.% Si. These values are in excellent accord with the reported values (1355°C and 90.7 At.% Si) by Lundin et al.[10] and Kieffer[11].

Figure 21 shows the experimentally determined melting points, qualitative X-ray findings of solid-state samples in the Zr-Si system, and Figure 22 depicts the assembled phase diagram of this system.

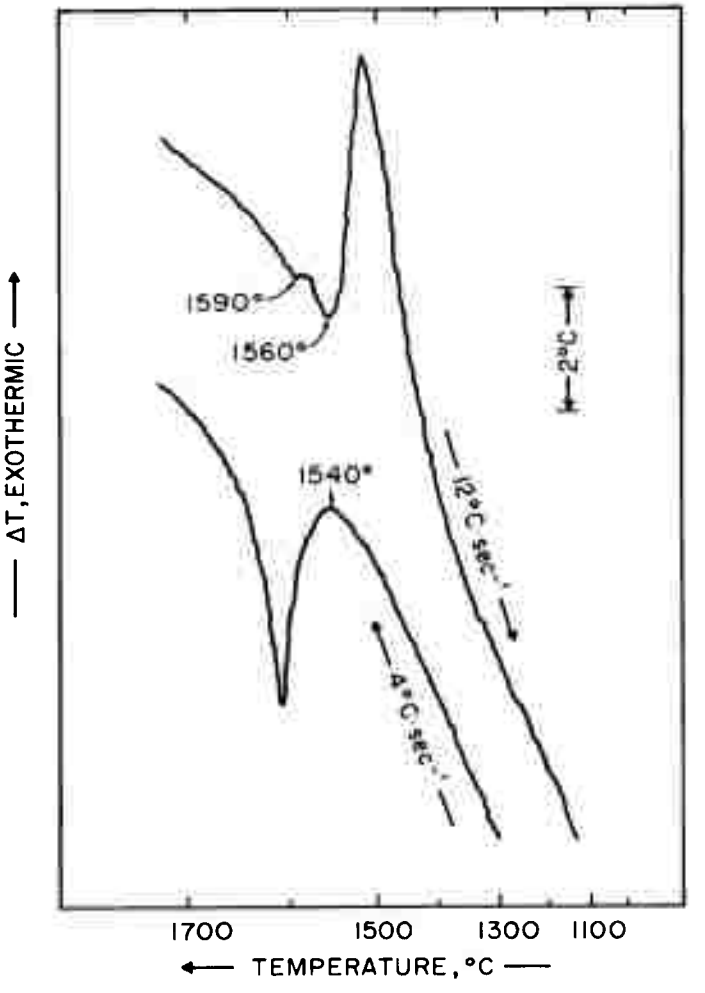

Figure 16. DTA Thermogram of a Zr-Si 48.5-51.5 Alloy Showing α-β Transformation of the ZrSi Phase. Slight Thermal Arrest Above Transformation Temperature is Due to the Silicon-Richer Peritectic Reaction.

Figure 17. Zr-Si: An Arc Melted 33.3-66.7 Alloy. X250

Primary β-ZrSi (Light, Smooth Grey) Surrounded by Peritectic Walls of $ZrSi_2$ (Darker Grey with Slight Cracks) in a Silicon-Richer Rest Melt.

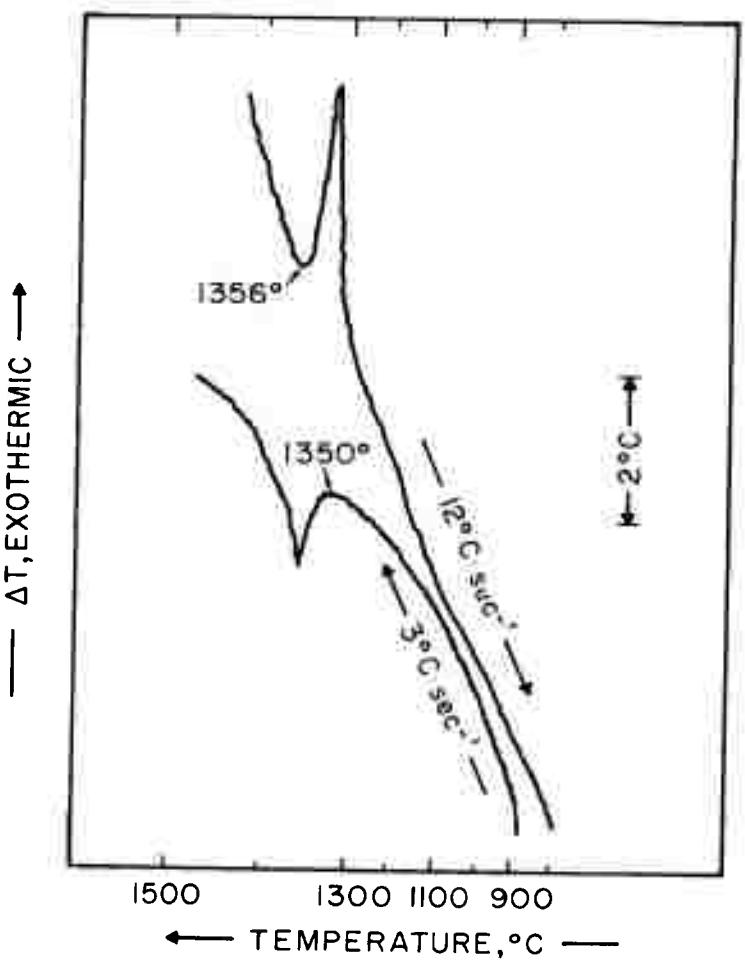

Figure 18. DTA Thermogram of a Zr-Si 10-90 Alloy Showing Eutectic Melting and Solidification.

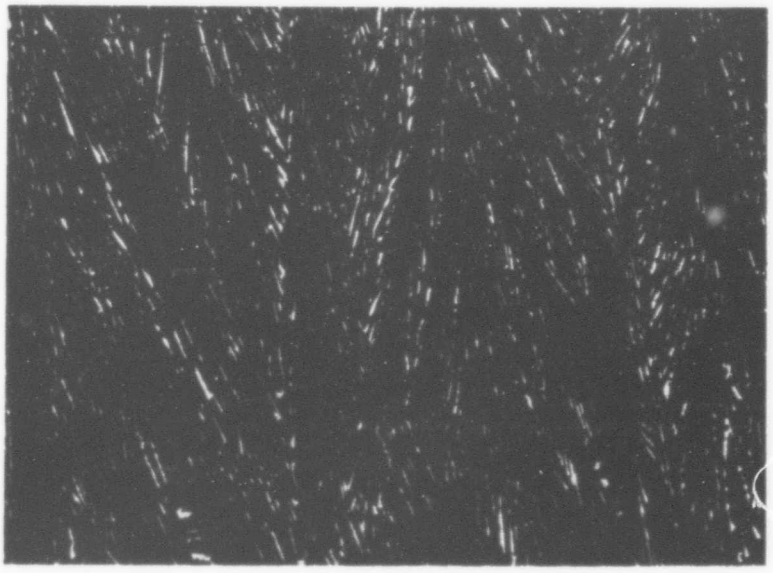

Figure 19. Zr-Si: An Arc Melted 10-90 Alloy. X250

$ZrSi_2$-Si Eutectic.

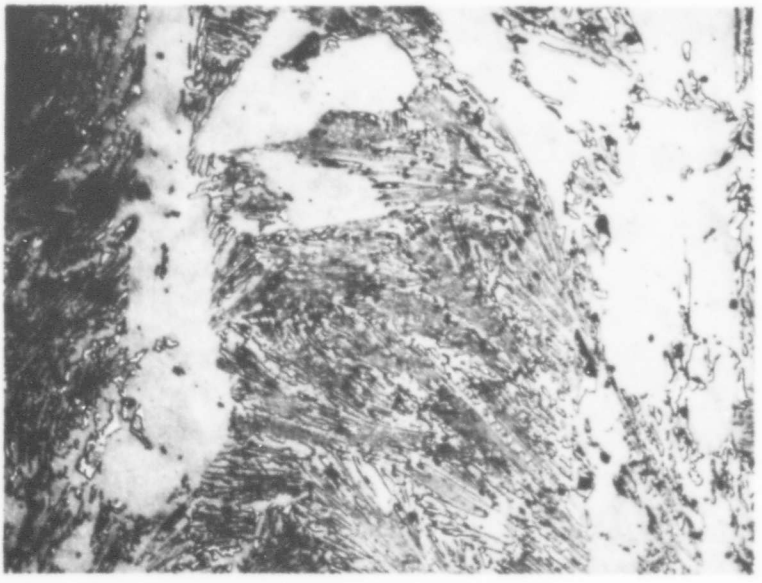

Figure 20. Zr-Si: An Arc Melted 8-92 Alloy. X225

Primary Si in a $ZrSi_2$-Si Matrix.

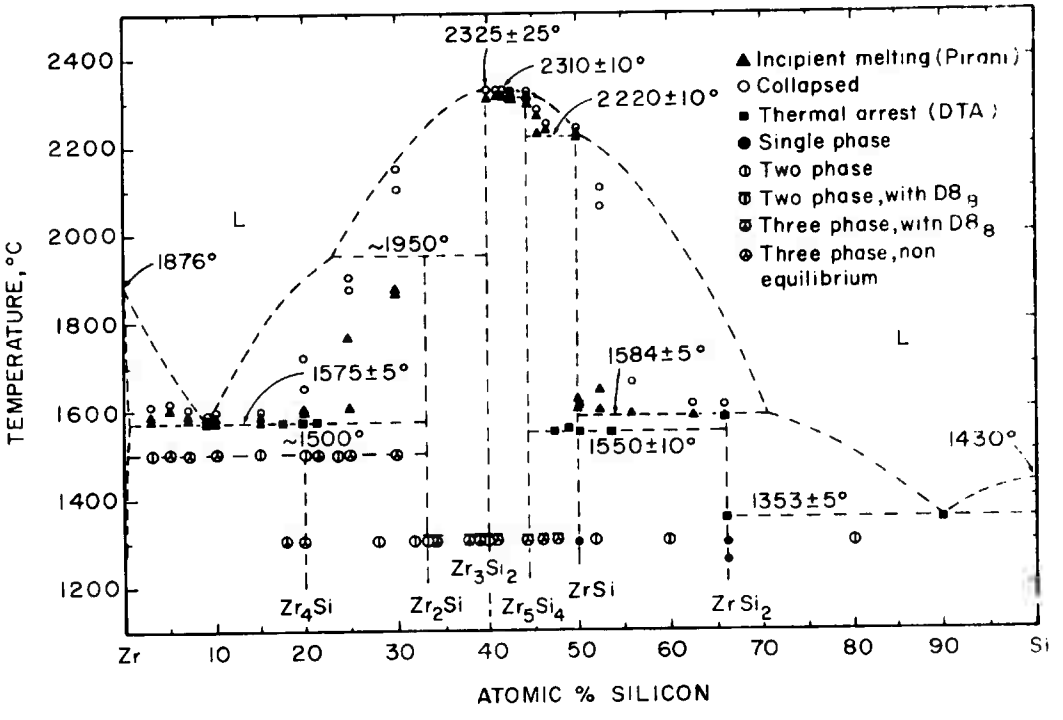

Figure 21. Zr-Si: Experimental Melting Points, Thermal Arrests, and Qualitative Solid State X-Ray Results in the Zr-Si System.

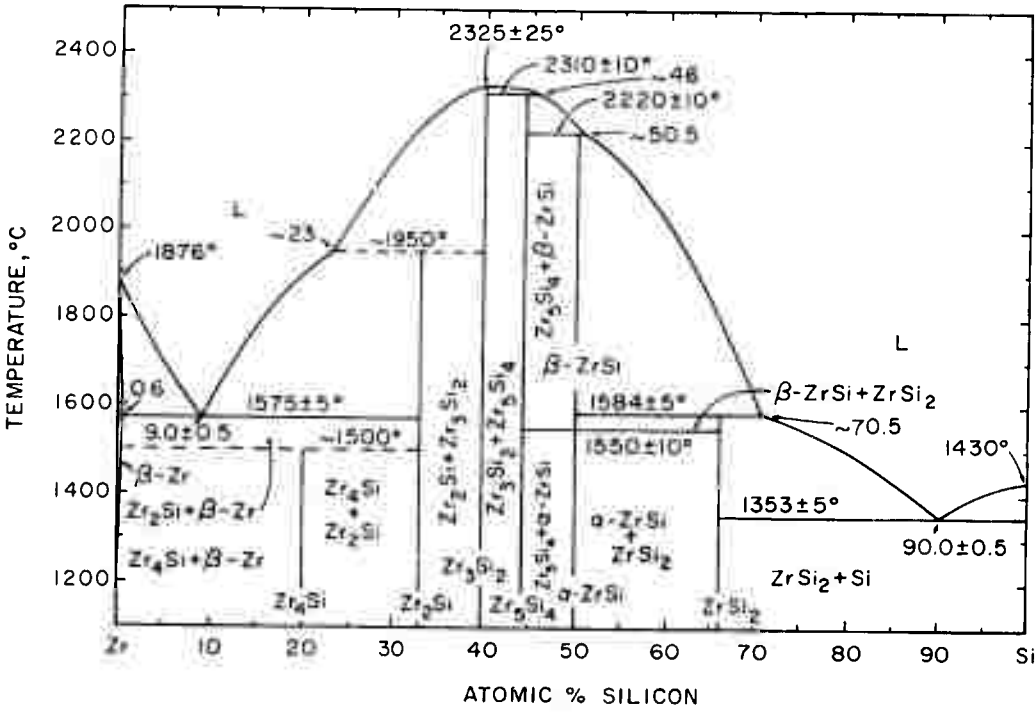

Figure 22. Zr-Si: Constitution Diagram.

B. THE HAFNIUM-SILICON SYSTEM

The difficulties observed in the interpretation of the equilibria in the region between 25 and about 43 atomic percent silicon in the zirconium-silicon system were also present in the hafnium-silicon system, but to a much lesser degree. That is, the quantity of ternary Hf_5Si_3 (C, N, O)-$D8_8$ phase present in samples from this region was able to be reduced by careful arc melting to an amount which enabled accurate interpretation of the phase equilibria by metallographic means. In fact, the amount of the ternary stabilized phase present in cold pressed and heat treated melting point samples was not large enough to obscure the peritectic decomposition isotherm of the Hf_2Si phase as is the case in the Zr-Si system. Not only is the ternary phase less easily stabilized in the Hf-Si system[33], whether the stabilizer be carbon, oxygen, nitrogen or boron, but also, the somewhat higher melting temperatures in the region about 40 At.% Si in the hafnium-silicon system, compared with the zirconium-silicon system, permit a better purification of the hafnium-silicon alloys, in this region, by arc melting.

The solubility of silicon in β-hafnium was investigated by metallography; X-ray techniques are quite insensitive when very small amounts of a second phase are involved.

An arc melted sample with 3 At.% silicon showed the primary crystallized β-Hf with sizeable amounts of β-Hf-Hf_2Si eutectic in the grain boundaries. The arc melted sample with 1 At.% silicon (Figure 23) still showed a small amount of Hf_2Si on the grain boundaries, indicating that the solubility of silicon in β-Hf at the eutectic temperature is less than 1 At.% silicon and probably of the order of 0.5 At.%. The solubility of silicon in the low temperature modification of hafnium, (α), was not specifically investigated, but assumed to also be of the order 0.5 At.% or less.

Neither the differential nor derivative thermal analysis experiments indicated a thermal arrest which would be attributed to a eutectoid reaction or peritectoid decomposition isotherm in the binary region stemming

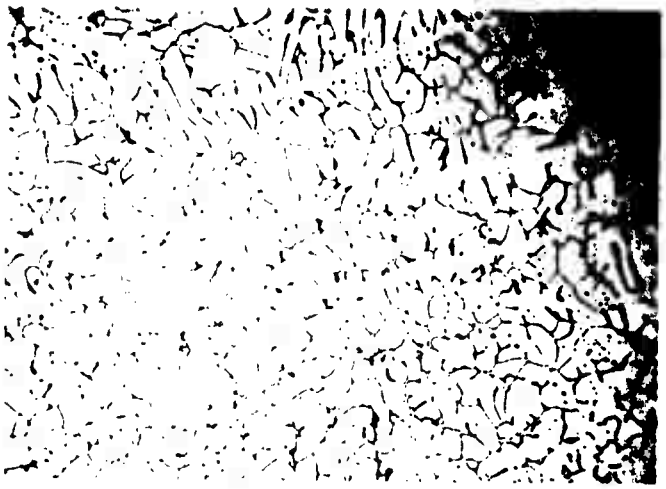

Figure 23. Hf-Si: An Arc Melted 99-1 Alloy. X400

Primary β-Hf (Transformed) with Small Amounts of Hf_2Si on the Grain Boundaries.

from the α-β transformation in hafnium; to indicate this temperature and mode uncertainty, a peritectoid isotherm is drawn in as a dashed line at about 1770°C (Figure 39).

The temperature of the β-Hf-Hf_2Si eutectic was measured on seven melting point and one derivative thermal analysis samples in the range from 5 to 30 At.% Silicon (Figures 38 and 24). The eutectic temperature determined was 1831 ± 5°C.

By means of metallography, (Figures 25, 26, and 27) the eutectic point was located quite close to 12 At.% silicon.

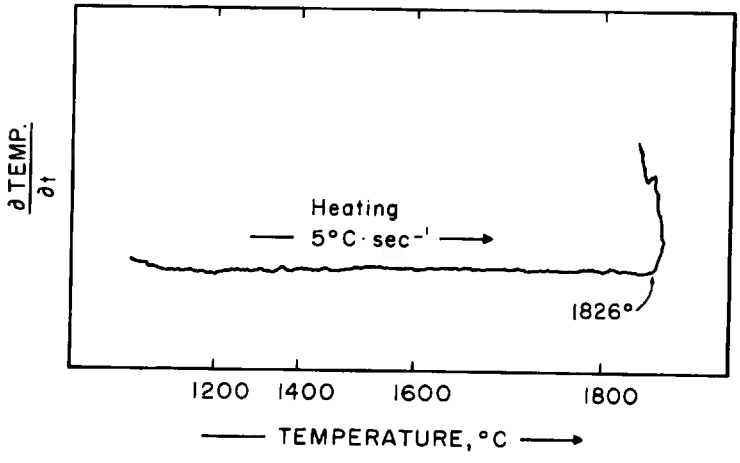

Figure 24. Derivative Thermogram of a Hf-Si 75-25 Alloy Showing Eutectic Melting.

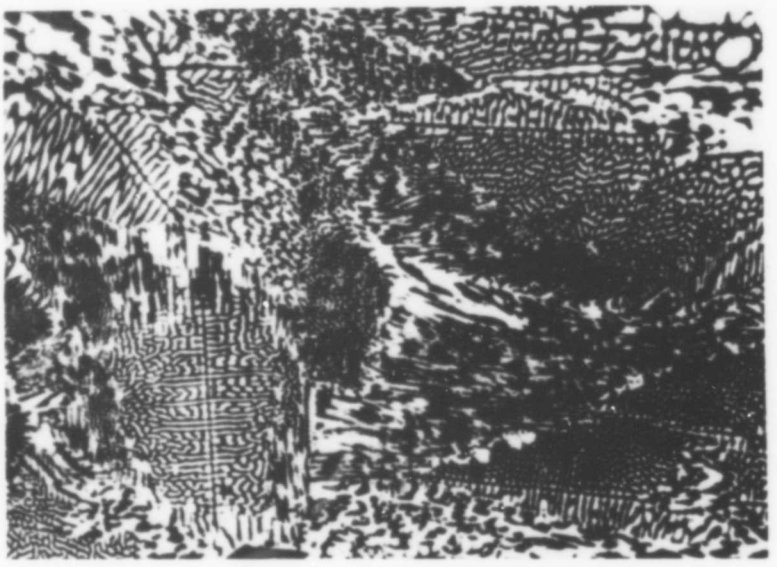

Figure 25. Hf-Si: An Arc Melted 87-13 Alloy, Eutectic Portion. X1000

β-Hf(Transformed) - Hf_2Si Eutectic.

Figure 26. Hf-Si: An Arc Melted 87-13 Alloy X1000

Primary Hf_2Si Grains (White) in a Partially Divorced β-Hf(Transformed)-Hf_2Si Eutectic.

Figure 27. Hf-Si: An Arc Melted 86.3-13.7 (Anal.) Alloy. X450

Primary Hf_2Si in a β -Hf(Transformed)-Hf_2Si Eutectic (Partially Divorced).

In contrast to the Zr-Si system, repeated experiments performed in the range of 17 to 22 At.% silicon showed that no other phase was formed either in arc melted or in long time heat treated (1300 and 1600°C) samples. In addition, no indication of the formation or decomposition of another phase in this region was detected by differential or derivative thermal analysis experiments. A phase, analogous to the Zr_4Si phase, or any other crystal structure does not occur in this region of the hafnium-silicon system.

The results of melting point measurements by the Pirani method in the region of 30 to about 40 At.% silicon show the typical run[30] of experimental points (Figure 38) for a peritectic reaction; the amount of liquid found in melting is proportionately small and the Pirani method shows varying incipient temperatures. A derivative thermal analysis run, however, yielded (Figure 28) results which indicate, in conjunction with the Pirani melting point experiments, that the peritectic temperature is 2083 $\pm$ 12°C.

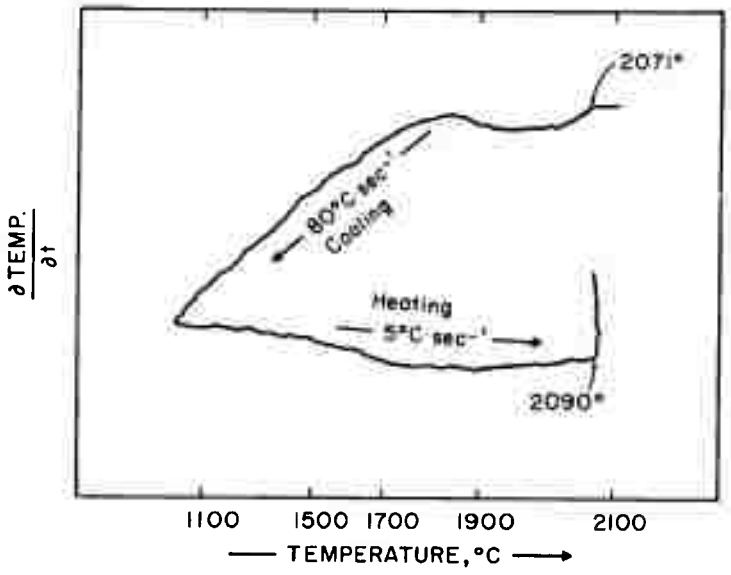

Figure 28. Derivative Thermogram of a Hf-Si 66.7-33.3 Alloy Showing Peritectic Melting and Solidification.

The metallography of the samples in this area showed, as in the case of the Zr-Si system, appreciable quantities of the ternary-stabilized $D8_8$ phase. The elimination of the $D8_8$ phase in Hf_2Si containing alloys was not possible even by careful arc melting, because the higher temperatures (>2400°), which appear necessary for arc melting purification of the Hf-Si alloys, are not obtained in the region of the peritectic decomposition of Hf_2Si (~2100°C).

Because of this effect, it was noticed, that the higher melting the alloys were in the Hf-Si system, the less $D8_8$ contaminate phase was present; only small amounts of the $D8_8$ phase were present in arc melted samples containing more than 40 At.% Si. In the central position of the diagram (45 to 50 At.% Si), the $D8_8$ phase was almost always present in large quantities in the X-ray patterns of samples which at some time in their heat treatment history, had been in the temperature range above about 1600°C, but, however, not arc melted. It was also observed that amount of $D8_8$ phase present in samples heat treated at 1300°C was quite small. It appears, then, as though the kinetics of formation of the $D8_8$ phase are favorable at higher temperatures, where, once the phase has scavanged all the carbon, oxygen, and nitrogen impurities from the silicon alloy, it becomes exceedingly difficult to rid the alloy of this ternary and higher order crystal structure except by arc melting at high temperatures in certain regions.

Furthermore, the observed changes in the lattice parameters of the $D8_8$ phase show a completely random course, independent of any zirconium or silicon content, in the area of about 23 to 55 At.% Si. It is apparent that the formation of the $D8_8$ phase in the binary Hf-Si system is completely dependent on the trace metalloid impurities present in each individual hafnium-silicon alloy. The $D8_8$ phase is not a binary constituent of the hafnium-silicon system.

A cursory analysis for carbon, nitrogen, and oxygen using a new Acton microprobe analyzer on a hafnium-silicon arc melted sample showing only Hf_3Si_2 and the $D8_8$ phase by both X-ray and metallographic examination proved too insensitive to detect the obviously trace quantities of metalloid contamination present.

The $D8_8$ phase, whose crystal structural composition is 37.5 At.% Si (with metalloid stabilizers) is always closely associated with the Hf_3Si_2 (40 At.%) compound in arc melted samples as also is the case in the Zr-Si system. In some metallographic instances it was seen that if the quantity of Hf_3Si_2 formed were small, or would be small, the $D8_8$ phase was found closely associated with or even occupying the place of the Hf_3Si_2.

This, in effect, explains the reasons for the difficulties in detecting and characterizing the Hf_3Si_2 phase which have existed for several years until 1961[16]. It was found that interpretations based, in part, on the assumption that the $D8_8$ phase were part of the Hf_3Si_2 compound, were helpful in interpretating the phase equilibria in the Hf-Si system.

Figure 29 shows a photomicrograph of a Hf-Si 69-32 alloy depicting a peritectic reaction. An X-ray of this arc melted alloy showed the presence of Hf_2Si, some α-Hf (transformed), some $D8_8$, and possible traces of Hf_3Si_2. The reaction depicted is the peritectic formation of Hf_2Si from $D8_8$ and melt, and rightly belongs to a ternary or higher order system; however, it is also used to illustrate the binary peritectic formation of Hf_2Si from Hf_3Si_2 and melt in the light of the above discussion.

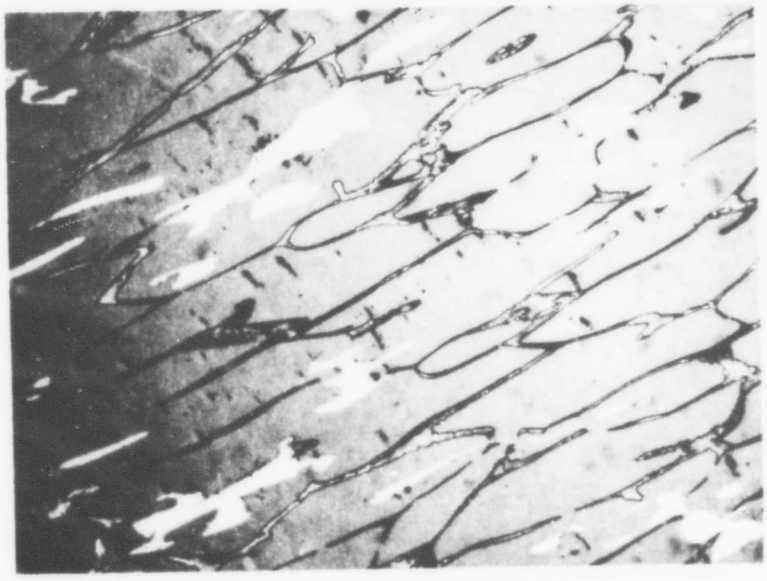

Figure 29. Hf-Si: An Arc Melted 68-32 Alloy X400

Primary Crystallized Ternary $D8_8$ Phase (White Grains with Some Small Cracks) Surrounded by Peritectic Walls of Hf_2Si with a Hafnium-Rich Melt [Rest β-Hf (Transformed)-Hf_2Si Eutectic Visible in Spots] on Grain Boundaries.

Examination of all the many Debye-Scherrer X-ray films of alloys containing the Hf_2Si phase, of arc melted, melting point, DTA, and heat treated samples showed that there was no change in the lattice parameters indicating that the Hf_2Si phase is essentially a line compound about the stoichiometric composition. The lattice parameters measured were $a = 6.54_7$ Å and $c = 5.19_0$ Å. These values are in good accord with literature values.

The highest melting, and only congruent melting compound in the Hf-Si system is the Hf_3Si_2 phase with a melting point of 2480 ± 20°C. Owing to the slight contamination effect of the $D8_8$ phase in this region, extremely sharp melting, one of the indications of a congruently melting compound, was not observed. In fact, metallographic specimens always showed amounts of the $D8_8$ phase accompanying the Hf_3Si_2 compound. However, no other compounds or reactions were observed in metallographic examination, and, owing to the small uncertainty of the melting point due to the $D8_8$ contamination, a congruent melting point of 2480 ± 20°C is assigned to the Hf_3Si_2 phase. Figure 30 shows the Hf_3Si_2 compound with some amounts of $D8_8$ phase as taken from an

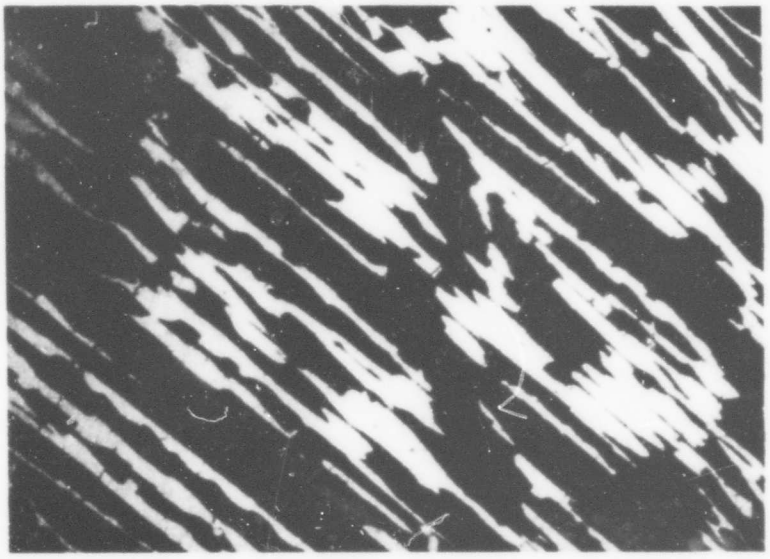

Figure 30. Hf-Si: An Arc Melted 60-40 Alloy X400

$D8_8$ Phase (Dark with Cracks) with Hf_3Si_2 (Light Grains).

arc melted sample. Again, as in the case of Hf_2Si, no change in lattice parameters for the Hf_3Si_2 could be detected; the lattice parameters of the tetragonal structure[16] are: a = 6.98$_2$ Å and c = 3.66$_3$ Å.

The Hf_5Si_4 phase, which had gone practically undetected and unclarified due to suppression by the $D8_8$ phase, has only an extremely narrow homogeneous range about the stoichiometric composition. Its lattice parameters, using the tetragonal structure clarified by Schubert[22] and Russian authors[23], are a = 7.02$_2$ Å and c = 12.88$_2$ Å. This compound decomposes peritectically at 2320 ± 15°C (Figures 38 and 39).

Figure 31 depicts the peritectic reaction mixture of Hf_3Si_2, Hf_5Si_4, some HfSi and small amounts of contaminate $D8_8$ phase.

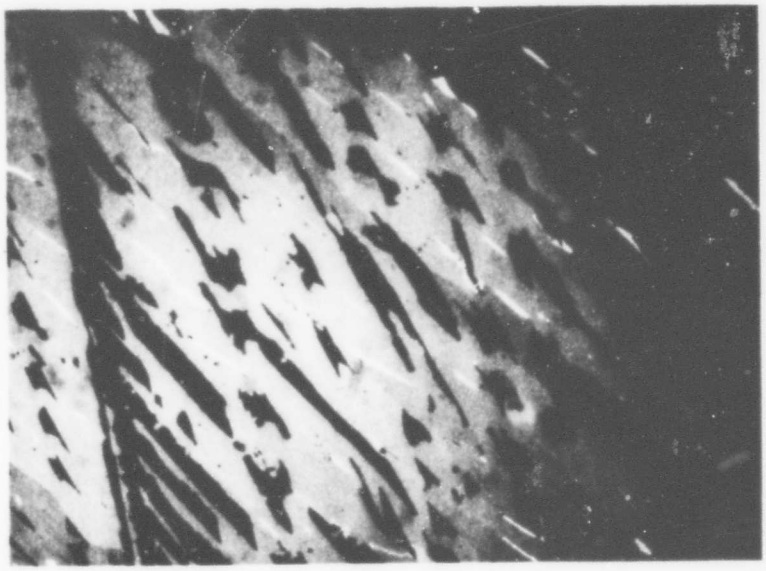

X400
(Polarized Light)

Figure 31. Hf-Si: An Arc Melted 57.5-42.5 Alloy

Peritectic Reaction Mixture Consisting of Hf_3Si_2 (Light Grey) and Hf_5Si_4 (White Grains) on Grain Boundaries. Interspersed Phase with Cracks is $D8_8$ Phase. The Peritectic Formation of Hf_5Si_4 has gone to Completion.

The HfSi equiatomic compound melts peritectically at 2142 ± 15°C to Hf_5Si_4 and melt (Figures 39 and 32) . Contrary to the characteristics of the ZrSi, which undergoes a structural transformation, the HfSi compound has the same crystal structure from about 1200°C up to its melting point. A derivative thermal analysis experiment on a Hf-Si 50-50 alloy yielded only the peritectic melting peak at 2138°C (Figure 33).

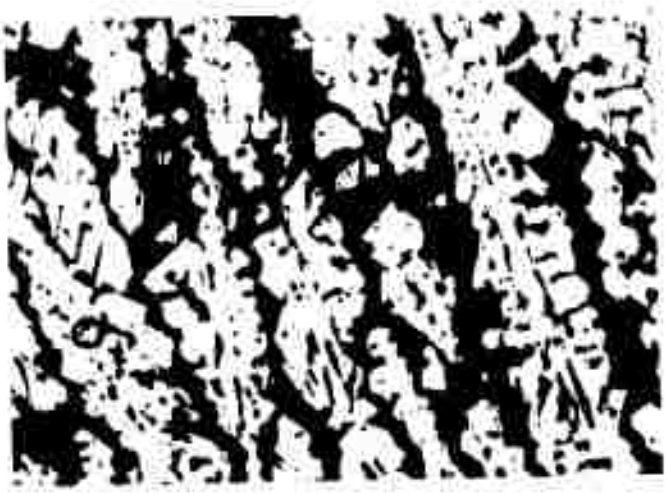

Figure 32. Hf-Si: An Arc Melted 50-50 Alloy X175

Primary Hf_5Si_4 Grains (Large White Chewed-up Dendrites) Surrounded by Peritectic Walls of HfSi (Grey). The Center of the HfSi Grains Contains Solidified Melt Consisting Primarily of $HfSi_2$ (Black, Etch Pitted).

No X-ray or metallographic evidence in any of the arc melted or heat treated HfSi-containing samples was found which would indicate that HfSi undergoes a transformation. Measurements of several X-ray films containing the pattern of HfSi in the orthorhombic structure[6] from arc melted and heat treated samples showed that within the measurement error limits, the lattice parameters with $a = 6.87_7$, $b = 3.77_0$, and $c = 5.22_9$ Å remain unchanged, indicating that HfSi has no appreciable homogeneous range.

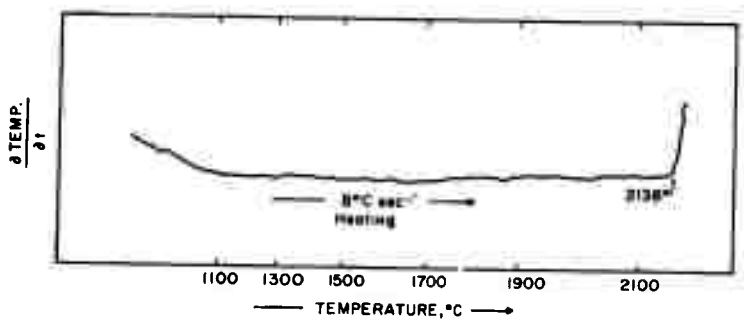

Figure 33. Derivative Thermogram of a Hf-Si 50-50 Alloy Showing Peritectic Melting.

The silicon-richest compound, $ZrSi_2$, also melts peritectically; the peritectic temperature is 1543 ± 8°C as determined by seven Pirani melting point samples along the peritectic isotherm (Figure 38). A photomicrograph showing the peritectic formation of $HfSi_2$ from HfSi and melt is shown in Figure 34. Similar to the other compounds in the Hf-Si system, $HfSi_2$ has no appreciable homogeneous range. The orthorhombic C49 crystal structure was measured, and the lattice parameters were: $a = 3.67_4$ Å, $b = 14.56$ Å, and $c = 3.63_1$ Å.

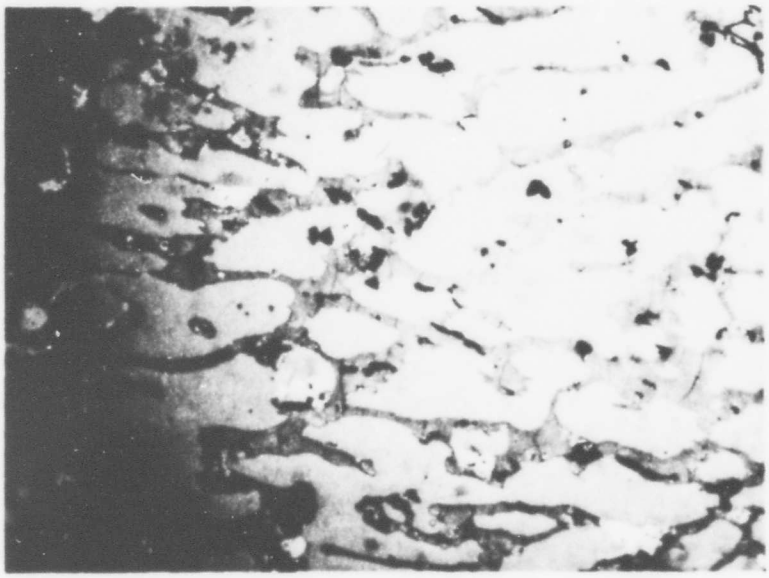

Figure 34. Hf-Si: An Arc Melted 40-60 Alloy X400

Primary HfSi (Large White Grains) Surrounded by Peritectic Walls of $HfSi_2$. In the Center of the $HfSi_2$ Portions are Silicon-Richer Melt Grains (Black) which have been Ripped out in Polishing.

Between $ZrSi_2$ and silicon there is a eutectic at 90 $\pm$ 1 At. % Si; the eutectic temperature (Figures 38 and 39), as measured by six Pirani melting point specimens is 1330 $\pm$ 8°C. Figures 35, 36, and 37 portray the metallographic findings of the alloys in this area.

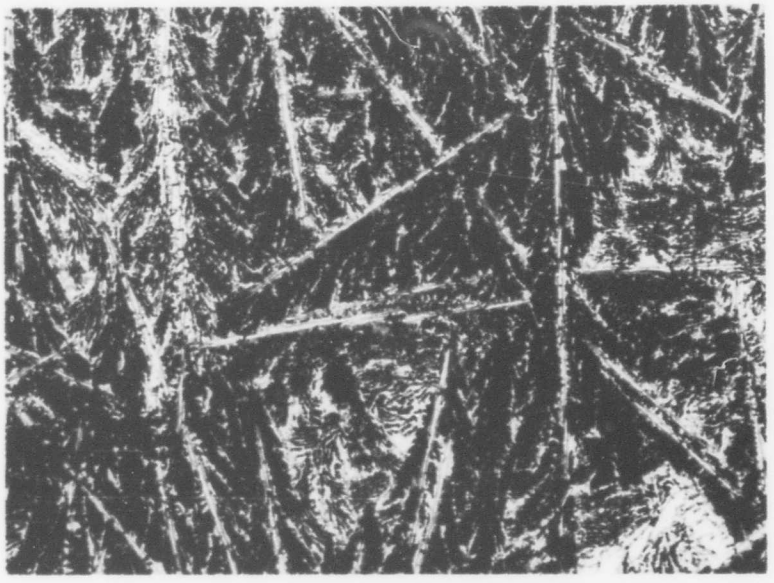

Figure 35. Hf-Si: An Arc Melted 10.5-89.5 Alloy X80

Primary $HfSi_2$ in a $HfSi_2$-Si Matrix.

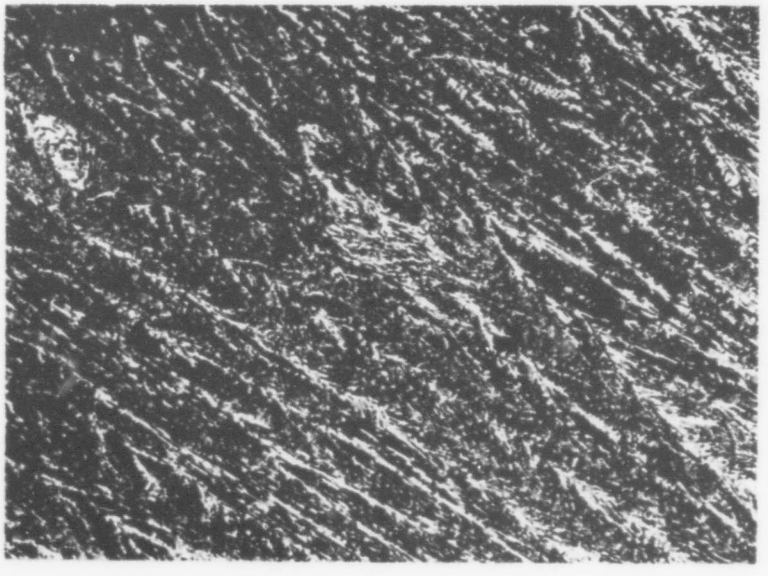

Figure 36. Hf-Si: An Arc Melted 10.2-89.8 (Anal.) Alloy X100
Eutectic Portion.

$HfSi_2$-Si Eutectic.

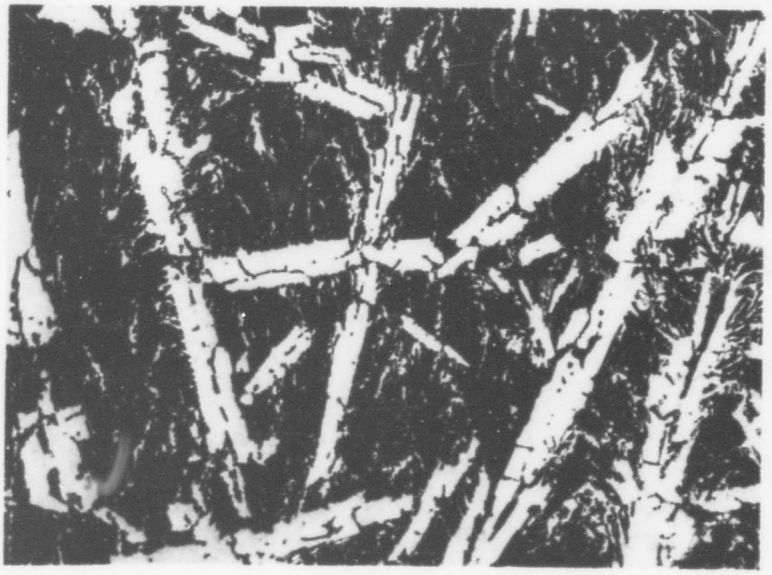

Figure 37. Hf-Si: An Arc Melted 7.2-92.8 (Anal.) Alloy X90

Primary Silicon in a $HfSi_2$-Si Eutectic Matrix.

The solubility of hafnium in silicon was not specifically investigated in this study, but is assumed to be negligible.

Figure 38 portrays the experimentally measured melting points, DTA thermal arrests, and qualitative solid state X-ray results, while Figure 39 shows the assembled phase diagram of the Hf-Si system based on experimental findings.

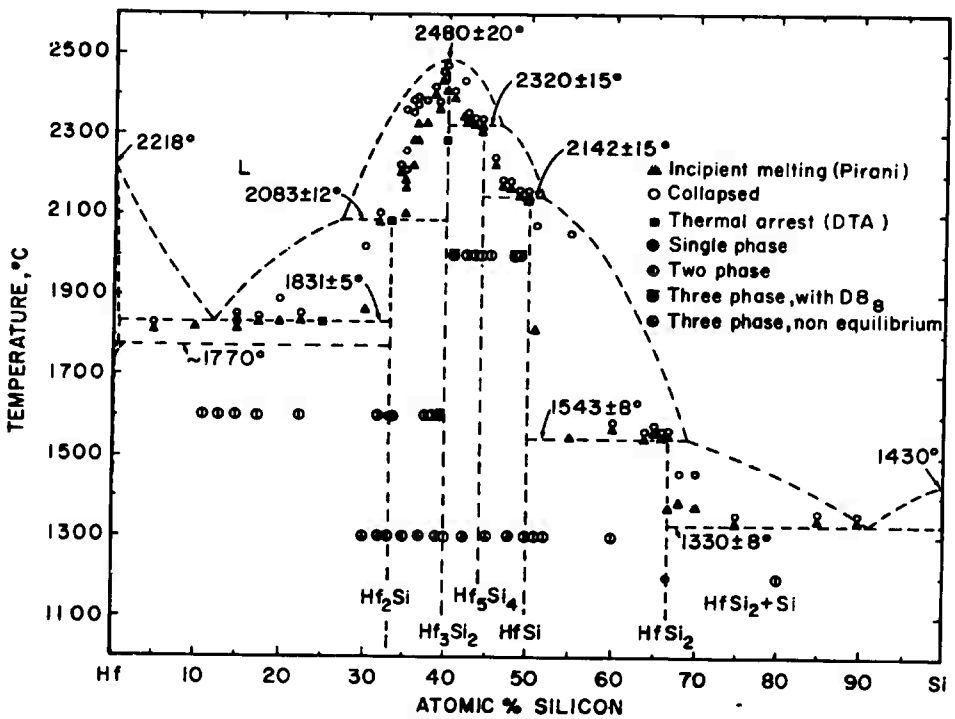

Figure 38. Experimental Melting Points, Thermal Arrests, and Qualitative Solid State X-Ray Results in the Hf-Si System.

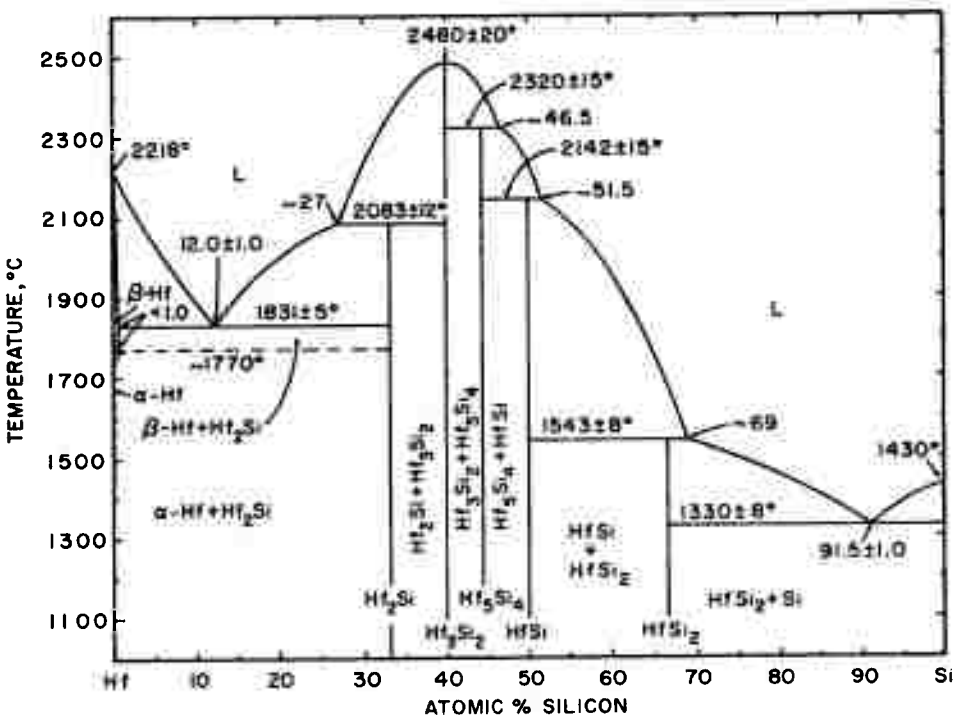

Figure 39. **Hf-Si: Constitution Diagram.**

V. DISCUSSION

The main contributing factor to the complexity of these two silicide systems, apart from the fact that there is a greater number of intermediate phases present than in most systems, is the occurrence of the impurity stabilized $D8_8$ phase which has clouded the majority of attempts of clarification of not only the phase equilibria, but also crystal structural behavior. This is evidenced by the complexity and confusion in reports published in the past as well as the difficulties encountered in this present investigation.

It seems as though the air alone, adsorbed on the surface of the various constituent powders used in typical metallurgical preparative techniques, is sufficient to stabilize the $D8_8$ crystal structure in the binary Hf-Si and Zr-Si systems when the alloys are subsequently heated to high temperatures. In addition, it may be that the normal amounts of oxygen and nitrogen (approx. 800 ppm) in solid solution in the "clean" elemental starting materials are also sufficient to stabilize the $D8_8$ crystal structure.

Perhaps a technique could be used to prepare cleaner alloys by arc melting of the elements prior to alloying, then alloying under arc melting, but in such a manner that the initial elemental buttons are not broken down to small particles permitting contaminate gasses to be adsorbed on the increased surface area. In this manner, the stabilizing contaminates would be eliminated before silicide alloying occurs.

REFERENCES

1. H. Seyfarth: Z. Krist. 67 (1928), 295.
2. St. v. Naray-Szabo: Z. Krist. A97 (1937), 223.
3. G. Brauer and A. Mitius: Z. anorg. Chem. 249 (1942), 338.
4. G. Brauer and H. Haag: unpublished work quoted by ref.(6).
5. P.G. Cotter, J.A. Kohn, and R.A. Potter: J.Amer.Ceram.Soc. 39 (1956), 11.
6. H. Schachner, H.Nowotny, and H. Kudielka: Mh.Chem. 85 (1954), 1140.
7. H. Schachner, H.Nowotny, and R.Machenschalk: Mh.Chem. 84 (1953), 677.
8. P. Pietrokowsky: Acta Cryst. 7 (1954), 435.
9. L. Brewer and O. Krikorian: AEC Publ. UCRL-2544 (1954).
10. E. Lundin, D.J. McPherson, and M.Hansen: Trans. ASM. 45 (1953), 901.
11. R. Kieffer, F. Benesovsky, and R. Machenschalk: Z.Metallkde. 45 (1954), 493.
12. H. Nowotny, B. Lux, and H. Kudielka: Mh.Chem. 87 (1956), 447.
13. L. Brewer and O. Krikorian: J. Electrochem. Soc. 103 (1956), 38.
14. P. Pietrokowsky: Quoted by Ref.(13).
15. C.H. Dauben: J. Electrochem. Soc. 104 (1957), 521.
16. O. Schob, H. Nowotny, and F. Benesovsky: Mh.Chem. 92 (1961), 1218.
17. O. Schob, H. Nowotny, and F. Benesovsky: Planseeber. 10 (1962), 65
18. K. Schubert, H.G. Meissner, and W. Rossteutscher: Naturwiss. 21 (1964), 506.
19. W. Rossteutscher and K. Schubert: Z. Metallkde, 56 (1965), 813.
20. A.G. Knapton: Nature 175 (1955), 730.
21. M.S. Farkas, A.A. Bauer, and R.F. Dickerson: Trans. ASM 53 (1961), 511.
22. H.U. Pfeifer and K. Schubert: Z.Metallkde 57 (1966), 884.

REFERENCES (cont'd)

23. O.G. Karpinskij and B.A. Evseev: An abstract in Moscow Abstracts A-82 (1966).

24. R. Kieffer and F. Benesovsky: Hartstoffe, Springer-Verlag, Vienna, Austria (1963), 474.

25. B. Post, F. Glaser, and D. Moskowitz: J.Chem. Phys. 22 (1954), 1264.

26. J.F. Smith and D.M. Bailey: Acta Cryst. 10 (1957), 341.

27. H. Nowotny, E. Laube, R. Kieffer and F. Benesovsky: Mh.Chem. 89 (1958), 701.

28. Lit. Cit. Ref (24), pp.474.

29. H. Nowotny, H. Braun, and F. Benesovsky: Radex Rundsch. (1960), 367.

30. E. Rudy, St. Windisch, and Y.A. Chang: AFML-TR-65-2, Part I, Vol.I (1965).

31. H.D. Heetderks, E. Rudy, and T. Eckert: AFML-TR-65-2, Part III, Vol. I (May 1965).

32. E.Rudy, St. Windisch, A.J. Stosick, and J.R. Hoffman: Trans. Met. Soc. AIME, 239 (1967), 1247.

33. C.E. Brukl: AFML-TR-65-2, Part II, Vol.X (Sept. 1966).

Unclassified
Security Classification

DOCUMENT CONTROL DATA - R&D

(Security classification of title, body of abstract and indexing annotation must be entered when the overall report is classified)

1. ORIGINATING ACTIVITY (Corporate author)
Materials Research Laboratory
Aerojet-General Corporation
Sacramento, California

2a. REPORT SECURITY CLASSIFICATION
Unclassified

2b. GROUP
N.A.

3. REPORT TITLE
Ternary Phase Equilibria in Transition Metal-Boron-Carbon-Silicon Systems
Part I. Finary Systems, Volume XIII. The Zirconium-Silicon and Hafnium-Silicon Systems

4. DESCRIPTIVE NOTES (Type of report and inclusive dates)
Documentary Report

5. AUTHOR(S) (Last name, first name, initial)
Brukl, C. E.

6. REPORT DATE	7a. TOTAL NO. OF PAGES	7b. NO. OF REFS
May 1968	60	33

8a. CONTRACT OR GRANT NO.	9a. ORIGINATOR'S REPORT NUMBER(S)
AF 33(615)-1249	AFML-TR-65-2 Part I, Volume XIII
b. PROJECT NO. 7350	
c. Task No. 735001	9b. OTHER REPORT NO(S) (Any other numbers that may be assigned this report)
d.	N.A.

10. AVAILABILITY/LIMITATION NOTICES
This document has been approved for public release and sale; its distribution is unlimited.

SUPPLEMENTARY NOTES	12. SPONSORING MILITARY ACTIVITY
	AFML (MAMC) Wright-Patterson AFB, Ohio 45433

13. ABSTRACT

The zirconium-silicon and hafnium-silicon binary systems have been investigated by means of Debye-Scherrer X-ray analysis, metallography, melting points, differential analysis techniques, and chemical analysis.

Both silicide systems contain a $D8_8$-type phase which is stabilized by trace impurities of oxygen and nitrogen.

The binary phases present are: Zr_4Si, Zr_2Si, Zr_3Si_2, Zr_5Si_4, α- and β-ZrSi, and $ZrSi_2$; in the hafnium system: Hf_2Si, Hf_3Si_2, Hf_5Si_4, and $HfSi_2$. The ZrSi phase undergoes an allotropic transformation at 1550°C; the high temperature form is of the CrB type while the low temperature crystal structure is of the FeB type.

Complete phase diagrams from 1100°C up to melting are given.

DD FORM 1 JAN 64 1473

Unclassified
Security Classification

14. KEY WORDS	LINK A		LINK B		LINK C	
	ROLE	WT	ROLE	WT	ROLE	WT
binary phase equilibria						
zirconium-silicon						
hafnium-silicon						
refractory alloys						

INSTRUCTIONS

1. **ORIGINATING ACTIVITY:** Enter the name and address of the contractor, subcontractor, grantee, Department of Defense activity or other organization *(corporate author)* issuing the report.

2a. **REPORT SECURITY CLASSIFICATION:** Enter the overall security classification of the report. Indicate whether "Restricted Data" is included. Marking is to be in accordance with appropriate security regulations.

2b. **GROUP:** Automatic downgrading is specified in DoD Directive 5200.10 and Armed Forces Industrial Manual. Enter the group number. Also, when applicable, show that optional markings have been used for Group 3 and Group 4 as authorized.

3. **REPORT TITLE:** Enter the complete report title in all capital letters. Titles in all cases should be unclassified. If a meaningful title cannot be selected without classification, show title classification in all capitals in parenthesis immediately following the title.

4. **DESCRIPTIVE NOTES:** If appropriate, enter the type of report, e.g., interim, progress, summary, annual, or final. Give the inclusive dates when a specific reporting period is covered.

5. **AUTHOR(S):** Enter the name(s) of author(s) as shown on or in the report. Enter last name, first name, middle initial. If military, show rank and branch of service. The name of the principal author is an absolute minimum requirement.

6. **REPORT DATE:** Enter the date of the report as day, month, year, or month, year. If more than one date appears on the report, use date of publication.

7a. **TOTAL NUMBER OF PAGES:** The total page count should follow normal pagination procedures, i.e., enter the number of pages containing information.

7b. **NUMBER OF REFERENCES:** Enter the total number of references cited in the report.

8a. **CONTRACT OR GRANT NUMBER:** If appropriate, enter the applicable number of the contract or grant under which the report was written.

8b, 8c, & 8d. **PROJECT NUMBER:** Enter the appropriate military department identification, such as project number, subproject number, system numbers, task number, etc.

9a. **ORIGINATOR'S REPORT NUMBER(S):** Enter the official report number by which the document will be identified and controlled by the originating activity. This number must be unique to this report.

9b. **OTHER REPORT NUMBER(S):** If the report has been assigned any other report numbers *(either by the originator or by the sponsor)*, also enter this number(s).

10. **AVAILABILITY/LIMITATION NOTICES:** Enter any limitations on further dissemination of the report, other than those imposed by security classification, using standard statements such as:

(1) "Qualified requesters may obtain copies of this report from DDC."

(2) "Foreign announcement and dissemination of this report by DDC is not authorized."

(3) "U. S. Government agencies may obtain copies of this report directly from DDC. Other qualified DDC users shall request through _____."

(4) "U. S. military agencies may obtain copies of this report directly from DDC. Other qualified users shall request through _____."

(5) "All distribution of this report is controlled. Qualified DDC users shall request through _____."

If the report has been furnished to the Office of Technical Services, Department of Commerce, for sale to the public, indicate this fact and enter the price, if known.

11. **SUPPLEMENTARY NOTES:** Use for additional explanatory notes.

12. **SPONSORING MILITARY ACTIVITY:** Enter the name of the departmental project office or laboratory sponsoring *(paying for)* the research and development. Include address.

13. **ABSTRACT:** Enter an abstract giving a brief and factual summary of the document indicative of the report, even though it may also appear elsewhere in the body of the technical report. If additional space is required, a continuation sheet shall be attached.

It is highly desirable that the abstract of classified reports be unclassified. Each paragraph of the abstract shall end with an indication of the military security classification of the information in the paragraph, represented as *(TS), (S), (C), or (U).*

There is no limitation on the length of the abstract. However, the suggested length is from 150 to 225 words.

14. **KEY WORDS:** Key words are technically meaningful terms or short phrases that characterize a report and may be used as index entries for cataloging the report. Key words must be selected so that no security classification is required. Identifiers, such as equipment model designation, trade name, military project code name, geographic location, may be used as key words but will be followed by an indication of technical context. The assignment of links, rules, and weights is optional.